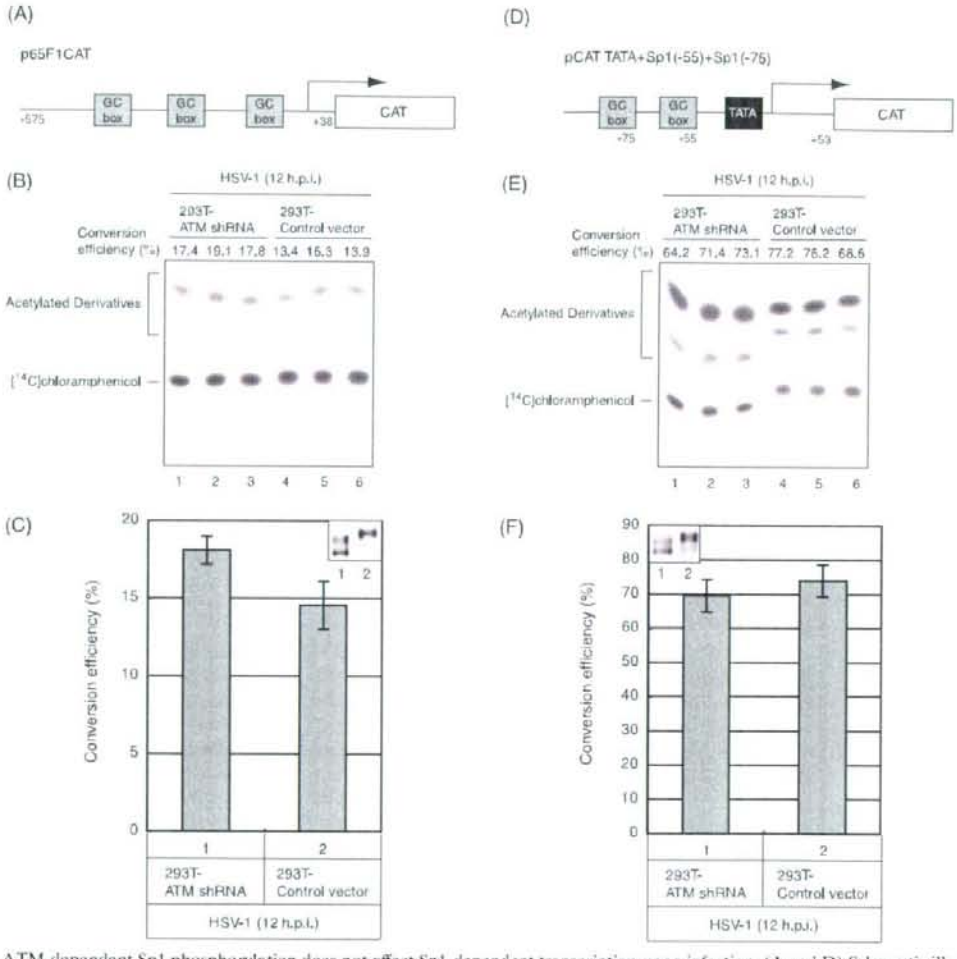


FIG. 9. ATM-dependent Sp1 phosphorylation does not affect Sp1-dependent transcription upon infection. (A and D) Schematic illustration of reporter vectors: p65F1CAT contains three Sp1-binding sites (GC-boxes) of the TATA less p65 promoter sequence (−575 to +38) (A), and pCAT TATA+Sp1(−55)+Sp1(−75) contains two GC-boxes and TATA consensus sequence of HCMV major immediate-early gene (D). (B and E) 293T-ATM shRNA and 293T-Control vector cells were transfected with either p65F1CAT (B) or pCAT TATA+Sp1(−55)+Sp1(−75) (E), infected with HSV-1 at 24 h posttransfection at an MOI of 5, and harvested at 12 hpi. CAT assays were performed as described in Materials and Methods. All transfection experiments were in triplicate. (C and F) Data from three independent experiments in panels B and E were plotted on the graph, respectively. The levels of activity (i.e., the conversion efficiency) were determined by calculating the percentage of the conversion of unacetylated [$^{14}$C]chloramphenicol to the acetylated form. In order to confirm phosphorylation states and amounts of Sp1 in 293T-ATM shRNA and 293T-Control vector cells infected with HSV-1 at 12 hpi, equal amounts of proteins from each sample were subjected to immunoblot analysis with anti-Sp1 antibody (panels C and F, inset images).

293T-ATM shRNA cells and 293T-Control vector cells (53). Thus, although at least Ser-56 and Ser-101 of Sp1 were phosphorylated dependent on ATM during HSV-1 infection, the Sp1 phosphorylation at both sites does not appear to affect Sp1-dependent transcriptional activity upon HSV-1 infection. Therefore, modification of Sp1 besides phosphorylation at Ser-56 and Ser-101 might induce the reduction of its transcriptional activity during the HSV-1 infection.

IR rapidly activates ATM, which then phosphorylates several transcription factors such as p53, ATF2, and CREB (4, 6, 51). In the present study, high doses of IR (10 and 20 Gy) induced the hyperphosphorylation of Sp1 in ATM expression-positive cells, but it did not so significantly in ATM expression-silenced cells (Fig. 4), suggesting that Sp1 is phosphorylated in an IR-induced ATM-dependent manner. A previous report demonstrated that IR at low dose (3 to 6 Gy) induces phosphorylation of Sp1 and simultaneously causes an increase in DNA-binding activity of Sp1 (40, 61). Furthermore, coexpression of Sp1 and ATM in *Drosophila* Schneider cells lacking endogenous Sp1 results in an ATM dose-dependent synergistic transactivation of IGF-IR promoter containing Sp1 binding sites, suggesting that Sp1 phosphorylation by ATM might in-

crease its transactivation activity (50). In the present study, however, the transcriptional activity from the Sp1 responsive promoter in ATM-silenced cells upon HSV-1 infection was almost the same as that in ATM-intact cells. Upon HSV-1 infection, Sp1 might undergo phosphorylation besides ATM-dependent phosphorylation or other modification(s). Thus, complex modification(s) of Sp1 caused by HSV-1 infection might mask the functional change by the phosphorylation at Ser-56 and Ser-101.

Kim and DeLuca (31) first documented the hyperphosphorylation of transcription factor Sp1 after HSV-1 infection. From studies conducted with ICP4 deletion mutants, these authors speculated that ICP4 is necessary for the hyperphosphorylation of Sp1 directly or indirectly. Also, they observed partial conversion of Sp1 to the hyperphosphorylated form during infection with wild-type HSV-1 in the presence of phosphonoacetic acid, a specific inhibitor of the viral DNA polymerase (31). We and others have previously demonstrated that HSV infection elicits ATM-dependent DNA damage responses, whereas infection with a UV-inactivated virus or with a replication-defective virus does not, suggesting that viral DNA synthesis is essential for ATM activation (37, 53). In the presence of phosphonoacetic acid, the ATM DNA damage signaling upon infection is blocked at a low multiplicity of infection, although the UL42 gene product, viral early protein, is expressed (37, 53). Therefore, ICP4 may indirectly contribute to Sp1 hyperphosphorylation through expression for viral replication proteins synthesizing viral DNA. Since synthesized viral DNA structure triggers activation of ATM-dependent DNA damage responses upon HSV infection, newly syhthesized viral DNA rather than expressed viral protein(s) appears to be necessary for the hyperphosphorylation of Sp1.

## ACKNOWLEDGMENTS

We thank G. Suske, Philipps-Universität, Marburg, Germany, for CMV-hSp1; M. B. Kastan, St. Jude Children's Research Hospital, for pcDNA-Flag-ATMwt and pcDNA-Flag-ATMkd; A. D. Yurochko, Louisiana State University Health Sciences Center, for p65F1CAT; W. Nakai, Osaka University (Japan), for pFastBac1 containing a sequence (RGS-6xHis-Flag); B. Roizman, The University of Chicago, for R7041 and R7356; M. Fujita and Y. Tatsumi, National Cancer Center Research Institute (Japan), for the 293T-ATM shRNA and 293T-Control vector cell lines; A. Kurimasa, Tottori University (Japan), for the M059J and MJ-M6 cell lines; and K. Ishizaki and H. Nakamura, Aichi Cancer Center Research Institute (Japan), for the AT10S/T-n cells. We also thank H. Goto and Y. Nishikawa, Aichi Cancer Center Research Institute (Japan), for instruction for the preparation of phosphopeptide-specific antibodies and for assistance with cell culture, respectively.

This study was supported by grants-in-aid for Scientific Research on Priority Areas from the Ministry of Education, Science, Sports, Culture, and Technology of Japan (19041078, 18012058, and 18390147 to T.T.) and partly by the Uehara Memorial Foundation. Y.S. and A.K. were supported by a Research Fellowship of the Japanese Society for the Promotion of Science for Young Scientists.

## REFERENCES

1. **Abraham, R. T.** 2001. Cell cycle checkpoint signaling through the ATM and ATR kinases. Genes Dev. **15**:2177–2196.
2. **Armstrong, S. A., D. A. Barry, R. W. Leggett, and C. R. Mueller.** 1997. Casein kinase II-mediated phosphorylation of the C terminus of Sp1 decreases its DNA binding activity. J. Biol. Chem. **272**:13489–13495.
3. **Bartek, J., and J. Lukas.** 2003. Chk1 and Chk2 kinases in checkpoint control and cancer. Cancer Cell **3**:421–429.
4. **Bhoumik, A., S. Takahashi, W. Breitweiser, Y. Shiloh, N. Jones, and Z. Ronai.** 2005. ATM-dependent phosphorylation of ATF2 is required for the DNA damage response. Mol. Cell **18**:577–587.
5. **Bouwman, P., and S. Philipsen.** 2002. Regulation of the activity of Sp1-related transcription factors. Mol. Cell Endocrinol. **195**:27–38.
6. **Canman, C. E., D. S. Lim, K. A. Cimprich, Y. Taya, K. Tamai, K. Sakaguchi, E. Appella, M. B. Kastan, and J. D. Siliciano.** 1998. Activation of the ATM kinase by ionizing radiation and phosphorylation of p53. Science **281**:1677–1679.
7. **Chen, B. P., N. Uematsu, J. Kobayashi, Y. Lerenthal, A. Krempler, H. Yajima, M. Lobrich, Y. Shiloh, and D. J. Chen.** 2007. Ataxia telangiectasia mutated (ATM) is essential for DNA-PKcs phosphorylations at the Thr-2609 cluster upon DNA double strand break. J. Biol. Chem. **282**:6582–6587.
8. **Chen, P., C. Luo, Y. Deng, K. Ryan, J. Register, S. Margosiak, A. Tempczyk-Russell, B. Nguyen, P. Myers, K. Lundgren, C. C. Kan, and P. M. O'Connor.** 2000. The 1.7-Å crystal structure of human cell cycle checkpoint kinase Chk1: implications for Chk1 regulation. Cell **100**:681–692.
9. **Chu, S., and T. J. Ferro.** 2005. Sp1: regulation of gene expression by phosphorylation. Gene **348**:1–11.
10. **Chun, H. H., R. B. Cary, F. Lansigan, J. Whitelegge, D. J. Rawlings, and R. A. Gatti.** 2004. ATM protein purified from vaccinia virus expression system: DNA binding requirements for kinase activation. Biochem. Biophys. Res. Commun. **322**:74–81.
11. **Chun, R. F., O. J. Semmes, C. Neuveut, and K. T. Jeang.** 1998. Modulation of Sp1 phosphorylation by human immunodeficiency virus type 1 Tat. J. Virol. **72**:2615–2629.
12. **Cortez, D., G. Glick, and S. J. Elledge.** 2004. Minichromosome maintenance proteins are direct targets of the ATM and ATR checkpoint kinases. Proc. Natl. Acad. Sci. USA **101**:10078–10083.
13. **Cortez, D., Y. Wang, J. Qin, and S. J. Elledge.** 1999. Requirement of ATM-dependent phosphorylation of brca1 in the DNA damage response to double-strand breaks. Science **286**:1162–1166.
14. **Courey, A. J., and R. Tjian.** 1988. Analysis of Sp1 in vivo reveals multiple transcriptional domains, including a novel glutamine-rich activation motif. Cell **55**:887–898.
15. **Dynan, W. S., and R. Tjian.** 1983. Isolation of transcription factors that discriminate between different promoters recognized by RNA polymerase II. Cell **32**:669–680.
16. **Dynan, W. S., and R. Tjian.** 1983. The promoter-specific transcription factor Sp1 binds to upstream sequences in the SV40 early promoter. Cell **35**:79–87.
17. **Fojas de Borja, P., N. K. Collins, P. Du, J. Azizkhan-Clifford, and M. Mudryj.** 2001. Cyclin A-CDK phosphorylates Sp1 and enhances Sp1-mediated transcription. EMBO J. **20**:5737–5747.
18. **Gaspar, M., and T. Shenk.** 2006. Human cytomegalovirus inhibits a DNA damage response by mislocalizing checkpoint proteins. Proc. Natl. Acad. Sci. USA **103**:2821–2826.
19. **Gidoni, D., W. S. Dynan, and R. Tjian.** 1984. Multiple specific contacts between a mammalian transcription factor and its cognate promoters. Nature **312**:409–413.
20. **Goldstein, D. J., and S. K. Weller.** 1988. Factor(s) present in herpes simplex virus type 1-infected cells can compensate for the loss of the large subunit of the viral ribonucleotide reductase: characterization of an ICP6 deletion mutant. Virology **166**:41–51.
21. **Gueven, N., K. Keating, T. Fukao, H. Loeffler, N. Kondo, H. P. Rodemann, and M. F. Lavin.** 2003. Site-directed mutagenesis of the ATM promoter: consequences for response to proliferation and ionizing radiation. Genes Chromosomes Cancer **38**:157–167.
22. **Hagen, G., S. Muller, M. Beato, and G. Suske.** 1994. Sp1-mediated transcriptional activation is repressed by Sp3. EMBO J. **13**:3843–3851.
23. **Haidweger, E., M. Novy, and H. Rotheneder.** 2001. Modulation of Sp1 activity by a cyclin A/CDK complex. J. Mol. Biol. **306**:201–212.
24. **Honess, R. W., and B. Roizman.** 1974. Regulation of herpesvirus macromolecular synthesis. I. Cascade regulation of the synthesis of three groups of viral proteins. J. Virol. **14**:8–19.
25. **Hoppe, B. S., R. B. Jensen, and C. U. Kirchgessner.** 2000. Complementation of the radiosensitive M059J cell line. Radiat. Res. **153**:125–130.
26. **Hung, J. J., Y. T. Wang, and W. C. Chang.** 2006. Sp1 deacetylation induced by phorbol ester recruits p300 to activate 12(*S*)-lipoxygenase gene transcription. Mol. Cell. Biol. **26**:1770–1785.
27. **Isomura, H., M. F. Stinski, A. Kudoh, T. Daikoku, N. Shirata, and T. Tsurumi.** 2005. Two Sp1/Sp3 binding sites in the major immediate-early proximal enhancer of human cytomegalovirus have a significant role in viral replication. J. Virol. **79**:9597–9607.
28. **Jackson, S. P., J. J. MacDonald, S. Lees-Miller, and R. Tjian.** 1990. GC box binding induces phosphorylation of Sp1 by a DNA-dependent protein kinase. Cell **63**:155–165.
29. **Jazayeri, A., J. Falck, C. Lukas, J. Bartek, G. C. Smith, J. Lukas, and S. P. Jackson.** 2006. ATM- and cell cycle-dependent regulation of ATR in response to DNA double-strand breaks. Nat. Cell. Biol. **8**:37–45.
30. **Kadonaga, J. T., K. R. Carner, F. R. Masiarz, and R. Tjian.** 1987. Isolation of cDNA encoding transcription factor Sp1 and functional analysis of the DNA binding domain. Cell **51**:1079–1090.
31. **Kim, D. B., and N. A. DeLuca.** 2002. Phosphorylation of transcription factor Sp1 during herpes simplex virus type 1 infection. J. Virol. **76**:6473–6479.
32. **Kozlov, S., N. Gueven, K. Keating, J. Ramsay, and M. F. Lavin.** 2003. ATP

activates ataxia-telangiectasia mutated (ATM) in vitro. Importance of autophosphorylation. J. Biol. Chem. **278:**9309–9317.
33. **Kudoh, A., M. Fujita, L. Zhang, N. Shirata, T. Daikoku, Y. Sugaya, H. Isomura, Y. Nishiyama, and T. Tsurumi.** 2005. Epstein-Barr virus lytic replication elicits ATM checkpoint signal transduction while providing an S-phase-like cellular environment. J. Biol. Chem. **280:**8156–8163.
34. **Kurimasa, A., S. Kumano, N. V. Boubnov, M. D. Story, C. S. Tung, S. R. Peterson, and D. J. Chen.** 1999. Requirement for the kinase activity of human DNA-dependent protein kinase catalytic subunit in DNA strand break rejoining. Mol. Cell. Biol. **19:**3877–3884.
35. **Lees-Miller, S. P., M. C. Long, M. A. Kilvert, V. Lam, S. A. Rice, and C. A. Spencer.** 1996. Attenuation of DNA-dependent protein kinase activity and its catalytic subunit by the herpes simplex virus type 1 transactivator ICP0. J. Virol. **70:**7471–7477.
36. **Leggett, R. W., S. A. Armstrong, D. Barry, and C. R. Mueller.** 1995. Sp1 is phosphorylated and its DNA binding activity down-regulated upon terminal differentiation of the liver. J. Biol. Chem. **270:**25879–25884.
37. **Lilley, C. E., C. T. Carson, A. R. Muotri, F. H. Gage, and M. D. Weitzman.** 2005. DNA repair proteins affect the lifecycle of herpes simplex virus 1. Proc. Natl. Acad. Sci. USA **102:**5844–5849.
38. **Luo, M. H., K. Rosenke, K. Czornak, and E. A. Fortunato.** 2007. Human cytomegalovirus disrupts both ataxia telangiectasia mutated protein (ATM)- and ATM-Rad3-related kinase-mediated DNA damage responses during lytic infection. J. Virol. **81:**1934–1950.
39. **McGeoch, D. J., M. A. Dalrymple, A. J. Davison, A. Dolan, M. C. Frame, D. McNab, L. J. Perry, J. E. Scott, and P. Taylor.** 1988. The complete DNA sequence of the long unique region in the genome of herpes simplex virus type 1. J. Gen. Virol. **69**(Pt. 7)**:**1531–1574.
40. **Meighan-Mantha, R. L., A. T. Riegel, S. Suy, V. Harris, F. H. Wang, C. Lozano, T. L. Whiteside, and U. Kasid.** 1999. Ionizing radiation stimulates octamer factor DNA binding activity in human carcinoma cells. Mol. Cell. Biochem. **199:**209–215.
41. **Milanini-Mongiat, J., J. Pouyssegur, and G. Pages.** 2002. Identification of two Sp1 phosphorylation sites for p42/p44 mitogen-activated protein kinases: their implication in vascular endothelial growth factor gene transcription. J. Biol. Chem. **277:**20631–20639.
42. **Myers, J. S., and D. Cortez.** 2006. Rapid activation of ATR by ionizing radiation requires ATM and Mre11. J. Biol. Chem. **281:**9346–9350.
43. **Nakamura, H., H. Fukami, Y. Hayashi, T. Kiyono, S. Nakatsugawa, M. Hamaguchi, and K. Ishizaki.** 2002. Establishment of immortal normal and ataxia telangiectasia fibroblast cell lines by introduction of the hTERT gene. J. Radiat. Res. **43:**167–174.
44. **Parkinson, J., S. P. Lees-Miller, and R. D. Everett.** 1999. Herpes simplex virus type 1 immediate-early protein vmw110 induces the proteasome-dependent degradation of the catalytic subunit of DNA-dependent protein kinase. J. Virol. **73:**650–657.
45. **Peng, Y., R. G. Woods, H. Beamish, R. Ye, S. P. Lees-Miller, M. F. Lavin, and J. S. Bedford.** 2005. Deficiency in the catalytic subunit of DNA-dependent protein kinase causes down-regulation of ATM. Cancer Res. **65:**1670–1677.
46. **Purves, F. C., R. M. Longnecker, D. P. Leader, and B. Roizman.** 1987. Herpes simplex virus 1 protein kinase is encoded by open reading frame US3 which is not essential for virus growth in cell culture. J. Virol. **61:**2896–2901.
47. **Purves, F. C., W. O. Ogle, and B. Roizman.** 1993. Processing of the herpes simplex virus regulatory protein alpha 22 mediated by the UL13 protein kinase determines the accumulation of a subset of alpha and gamma mRNAs and proteins in infected cells. Proc. Natl. Acad. Sci. USA **90:**6701–6705.
48. **Rajcani, J., V. Andrea, and R. Ingeborg.** 2004. Peculiarities of herpes simplex virus (HSV) transcription: an overview. Virus Genes **28:**293–310.
49. **Roizman, B.** 1996. The function of herpes simplex virus genes: a primer for genetic engineering of novel vectors. Proc. Natl. Acad. Sci. USA **93:**11307–11312.
50. **Shahrabani-Gargir, L., T. K. Pandita, and H. Werner.** 2004. Ataxia-telangiectasia mutated gene controls insulin-like growth factor I receptor gene expression in a deoxyribonucleic acid damage response pathway via mechanisms involving zinc-finger transcription factors Sp1 and WT1. Endocrinology **145:**5679–5687.
51. **Shi, Y., S. L. Venkataraman, G. E. Dodson, A. M. Mabb, S. LeBlanc, and R. S. Tibbetts.** 2004. Direct regulation of CREB transcriptional activity by ATM in response to genotoxic stress. Proc. Natl. Acad. Sci. USA **101:**5898–5903.
52. **Shiloh, Y.** 2003. ATM and related protein kinases: safeguarding genome integrity. Nat. Rev. Cancer **3:**155–168.
53. **Shirata, N., A. Kudoh, T. Daikoku, Y. Tatsumi, M. Fujita, T. Kiyono, Y. Sugaya, H. Isomura, K. Ishizaki, and T. Tsurumi.** 2005. Activation of ataxia telangiectasia-mutated DNA damage checkpoint signal transduction elicited by herpes simplex virus infection. J. Biol. Chem. **280:**30336–30341.
54. **Spengler, M. L., and M. G. Brattain.** 2006. Sumoylation inhibits cleavage of Sp1 N-terminal negative regulatory domain and inhibits Sp1-dependent transcription. J. Biol. Chem. **281:**5567–5574.
55. **Stevens, C., L. Smith, and N. B. La Thangue.** 2003. Chk2 activates E2F-1 in response to DNA damage. Nat. Cell. Biol. **5:**401–409.
56. **Tatsumi, Y., N. Sugimoto, T. Yugawa, M. Narisawa-Saito, T. Kiyono, and M. Fujita.** 2006. Deregulation of Cdt1 induces chromosomal damage without rereplication and leads to chromosomal instability. J. Cell Sci. **119:**3128–3140.
57. **Wagner, E. K., J. F. Guzowski, and J. Singh.** 1995. Transcription of the herpes simplex virus genome during productive and latent infection. Prog. Nucleic Acids Res. Mol. Biol. **51:**123–165.
58. **Westphal, C. H.** 1997. Cell-cycle signaling: Atm displays its many talents. Curr. Biol. **7:**R789–R792.
59. **Wilkinson, D. E., and S. K. Weller.** 2006. Herpes simplex virus type I disrupts the ATR-dependent DNA-damage response during lytic infection. J. Cell Sci. **119:**2695–2703.
60. **Wilkinson, D. E., and S. K. Weller.** 2004. Recruitment of cellular recombination and repair proteins to sites of herpes simplex virus type 1 DNA replication is dependent on the composition of viral proteins within prereplicative sites and correlates with the induction of the DNA damage response. J. Virol. **78:**4783–4796.
61. **Yang, C. R., C. Wilson-Van Patten, S. M. Planchon, S. M. Wuerzberger-Davis, T. W. Davis, S. Cuthill, S. Miyamoto, and D. A. Boothman.** 2000. Coordinate modulation of Sp1, NF-κB, and p53 in confluent human malignant melanoma cells after ionizing radiation. FASEB J. **14:**379–390.
62. **Yurochko, A. D., M. W. Mayo, E. E. Poma, A. S. Baldwin, Jr., and E. S. Huang.** 1997. Induction of the transcription factor Sp1 during human cytomegalovirus infection mediates upregulation of the p65 and p105/p50 NF-κB promoters. J. Virol. **71:**4638–4648.

INSTITUT PASTEUR

Microbes and Infection 9 (2007) 1434–1438

www.elsevier.com/locate/micinf

Original article

# Identification of proteins directly phosphorylated by UL13 protein kinase from herpes simplex virus 1

Risa Asai, Takashi Ohno, Akihisa Kato, Yasushi Kawaguchi*

*Division of Viral Infection, Department of Infectious Disease Control, International Research Center for Infectious Diseases, The Institute of Medical Science, The University of Tokyo, 4-6-1 Shirokanedai, Minato-ku, Tokyo 108-8639, Japan*

Received 5 June 2007; accepted 25 July 2007
Available online 31 July 2007

**Abstract**

Herpes simplex virus 1 (HSV-1) UL13 is a viral protein kinase that regulates optimal viral replication in cell cultures. Identification of substrates of protein kinases is a crucial step to elucidate the mechanism by which they function. Using our developed system to analyze the specific protein kinase activity of UL13, we have shown that UL13 protein kinase directly phosphorylates the viral proteins ICP22 and UL49 previously reported to be putative substrates. We also identified UL41 as a previously unreported and novel substrate of UL13. These data will serve as a basis to clarify the mechanism by which UL13 influences viral replication.


*Keywords:* Simplex virus; UL13 protein kinase; Phosphorylation

## 1. Introduction

Herpes simplex viruses (HSVs) are ubiquitous throughout the world and can cause a variety of diseases in humans, including mucocutaneous infections such as herpes genitalis and herpes labialis, potentially sight-impairing herpetic eye disease, and life-threatening herpes encephalitis or disseminated disease [1]. Of the more than 80 viral genes encoded by HSV, this report concerns a viral protein encoded by the HSV-1 *UL13* gene.

The HSV-1 UL13 is a serine/threonine protein kinase that is packaged in the tegument, a virion structural component located between the nucleocapsid and the envelope [2]. UL13 plays a role in viral replication in cell cultures, since UL13 deletion mutants exhibit impaired replication in cell cultures [2]. It is well known that phosphorylation of proteins by protein kinases is the most common and effective modification that changes the activity of the target proteins. Phosphorylation of target proteins by specific protein kinases regulates many cellular functions such as transcription, translation, cell cycle regulation, protein degradation, and apoptosis [3,4]. Conceivably, HSV utilizes UL13 to regulate its own replicative process and to modify cellular machinery through the phosphorylation of viral and cellular proteins. In fact, UL13 has been reported to play multiple roles in viral gene expression, apoptosis, and nuclear egress [5–7].

UL13 may function by phosphorylating specific viral and cellular protein substrates. Identification of these substrates is a key step for clarification of the mechanisms by which UL13 regulates viral gene expression, apoptosis, and progeny virus egress, and for elucidation of other possible UL13 function(s). Thus far, numerous putative substrates for UL13 including ICP22, Us1.5, ICP0, gI/gE, UL47, UL49, UL13, p60, elongation factor 1δ (EF-1δ), casein kinase IIβ (CKIIβ), RNA polymerase II (RNA pol II), and Us3 have been reported based on the following observations. The phosphorylation and/or posttranslational processing of ICP22, Us1.5, ICP0, gI/gE, UL49, p60, EF-1δ, and RNA pol II have been demonstrated to

*Abbreviations:* HSV, herpes simplex virus; EF-1δ, elongation factor 1 delta; RNA pol II, RNA polymerase II; MBP, maltose binding protein; GST, glutathione-*S*-transferase; CBB, Coomassie brilliant blue.

* Corresponding author. Tel.: +81 3 6409 2070; fax: +81 3 6409 2072.
*E-mail address:* ykawagu@ims.u-tokyo.ac.jp (Y. Kawaguchi).

1286-4579/$ - see front matter © 2007 Elsevier Masson SAS. All rights reserved.
doi:10.1016/j.micinf.2007.07.008

be reduced or obviated in cells infected with UL13 mutant viruses [6,8–15], indicating that UL13 mediates the phosphorylation of the putative substrates in infected cells. However, in the experiments with UL13 mutant viruses, UL13 may have directly phosphorylated the putative substrates, or it may have either activated or induced other protein kinase(s) that phosphorylated these putative substrates. Therefore, it is necessary to demonstrate that the substrate is specifically and directly phosphorylated by the enzyme *in vitro*. Two methods have been reported to show that substrates are phosphorylated by UL13 *in vitro*. First, ICP0 and gI/gE have been shown to be phosphorylated by UL13 using immunoprecipitation with a polyclonal antibody to UL13 [13,14]. In these *in vitro* kinase assays, however, it is possible that the protein kinase activity detected using UL13 immunoprecipitation is due to a contaminating kinase(s) either associated with Us3 or coprecipitated by the antibody. Recently, we developed a more reliable system to analyze the specific protein kinase activity of UL13 *in vitro* [16]. In this system, we express large amounts of recombinant UL13 fused to glutathione *S*-transferase (GST) in insect cells using a recombinant baculovirus to obtain highly purified UL13 with enzymatic activity (Fig. 1). We also generated a kinase-negative mutant of UL13 in which the invariant lysine 176 was substituted with methionine to eliminate the possibility that kinase activity detected using purified recombinant UL13 is caused by kinase contamination during purification. The use of purified recombinant UL13 and its mutant for in vitro kinase assays enables us to examine a more specific activity of UL13 than that observed during UL13 immunoprecipitation with a polyclonal antibody. In fact, we previously demonstrated that a cellular protein Bid was not phosphorylated directly by Us3, another protein kinase encoded by HSV-1, in an assay system of Us3 kinase activity that used recombinant GST-Us3 and its kinase-negative mutant, even though it has been reported that Bid is efficiently phosphorylated by Us3 immunoprecipitates [17]. Using our developed system, we have shown that EF-1δ and Us3 are phosphorylated directly by UL13 *in vitro*. Among the numerous putative UL13 substrates reported to date, only EF-1δ and Us3 have been convincingly demonstrated to be phosphorylated directly by UL13 [6,16] and it is unknown at present whether the other reported putative substrates are directly phosphorylated by UL13. In the present study, we examined whether the putative UL13 substrates reported earlier are phosphorylated directly by UL13. We also attempted to identify a previously unreported novel substrate of UL13.

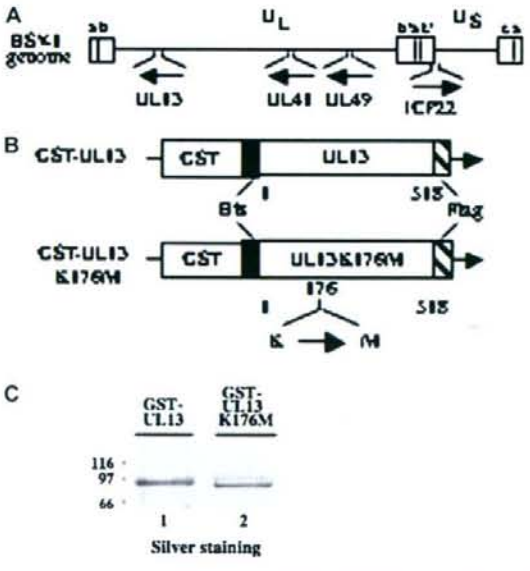


Fig. 1. (A) Schematic diagram of the genome structures of HSV-1 and the location of the *UL13*, *UL41*, *UL49* and *ICP22* genes. (B) Schematic diagram of the predicted amino acid sequence of GST-UL13 and its kinase-negative mutant GST-UL13K176M. The K176M mutation is indicated. (C) A silver-staining gel of purified GST-UL13 (lane 1) and GST-UL13K176M (lane 2) used in the *in vitro* kinase assays.

## 2. Materials and methods

### 2.1. Cells and viruses

*Spodoptera frugiperda* Sf9 cells were described previously [16,18]. The recombinant baculoviruses Bac-GST-UL13 and Bac-GST-UL13K176M were described previously [16].

### 2.2. Plasmids

pMAL-ICP22 was described previously [17]. pMAL-UL41 was constructed by amplifying the entire coding sequence of UL41 from pBC1007 [19] and cloning the DNA fragments into pMAL-c (New England BioLabs) in frame with the maltose binding protein (MBP). pMAL-UL41N and pMAL-UL41C were generated by amplifying the domain containing UL49 codons 1–246 and 215–489, respectively, by PCR from pBC1007 and cloning the DNA fragments into pMAL-c. pMAL-UL49N and pMAL-UL49C were generated by amplifying the domain containing UL49 codons 1–100 and 166–301, respectively, by PCR from pBC1007 and cloning the DNA fragments into pMAL-c. To generate pMAL-ARF6, the entire coding sequence of ARF6 was amplified by PCR from an Epstein–Barr virus-transformed human peripheral blood lymphocyte cDNA library (Clontech) and cloned into pMAL-c. ARF6 is a brefeldin A-insensitive member of the adenosine diphosphate (ADP) – ribosylation factor (Arf) family is a group of structurally related proteins that form a subset of the Ras superfamily of regulatory GTP-binding proteins [20–23].

### 2.3. Production and purification of MBP fusion proteins expressed in Escherichia coli

MBP fusion proteins (MBP-ICP22, MBP-UL41, MBP-UL41N, MBP-UL41C, MBP-UL49N, MBP-UL49C and MBP-ARF6) were expressed in *Escherichia coli* (*E. coli*) that had been transformed with pMAL-ICP22, pMAL-UL41, pMBP-UL41N,

pMBP-UL41C, pMBP-UL49N, pMBP-UL49C and pMBP-ARF6, respectively, and purified as described previously [16].

### 2.4. Purification of GST fusion protein from baculovirus-infected cells

GST-UL13 and GST-UL13K176M proteins were purified from Sf9 cells infected with Bac-GST-UL13 and Bac-GST-UL13K176M, respectively, as described previously [16].

### 2.5. In vitro kinase assays and phosphatase treatment

MBP fusion proteins were captured on amylose beads (New England BioLabs) and used as substrates for *in vitro* kinase assays with GST-UL13 and GST-UL13K176M as described previously [16]. The purified GST-UL13 and GST-UL13K176M used in the *in vitro* kinase assays were electrophoretically separated in a denaturing gel and are shown in Fig. 1C. After the *in vitro* kinase assays, the MBP fusion proteins captured on amylose beads were subjected to phosphatase treatment as described previously [17,19].

## 3. Results

### 3.1. UL13 directly phosphorylates ICP22 and UL49 in vitro

We examined whether the putative substrates reported earlier (ICP22 and UL49) were in fact directly phosphorylated by UL13 *in vitro*. ICP22 has been suggested to be a regulator of viral and cellular gene expression, while UL49 is among the most abundant of the tegument proteins. As substrates for these studies, we generated and purified chimeric proteins consisting of MBP fused to the putative substrates (MBP-ICP22, MBP-UL49N and MBP-UL49C). We also used the MBP-ARF6 protein as a control. As kinases for our studies, we used purified UL13 fused to GST (GST-UL13) from Sf9 cells infected with a recombinant baculovirus Bac-GST-UL13. We also used the kinase-negative mutant GST-UL13K176M as a control. The MBP fusion proteins were captured on amylose beads and used as substrates for *in vitro* kinase assays with GST-UL13 and GST-UL13K176M. In these assays, MBP-ICP22, MBP-UL49N, and MBP-UL49C proteins were labeled with [$\gamma$-$^{32}$P]ATP by purified GST-UL13, but MBP-ARF6 was not (Figs. 2B and 3C). When the kinase-negative mutant GST-UL13K176M was used instead of GST-UL13 in the assays, none of the MBP fusion proteins were labeled. Furthermore, labeling of the MBP fusion proteins by GST-UL13 was eliminated by phosphatase treatment (Figs. 2D and 3E). The expression of each MBP fusion protein and identification of each radiolabeled MBP protein band was verified by Coomassie brilliant blue (CBB) staining as shown in Fig. 2A,C and Fig. 3B,D. These results indicate that UL13 specifically and directly phosphorylates ICP22 and UL49 proteins *in vitro*.

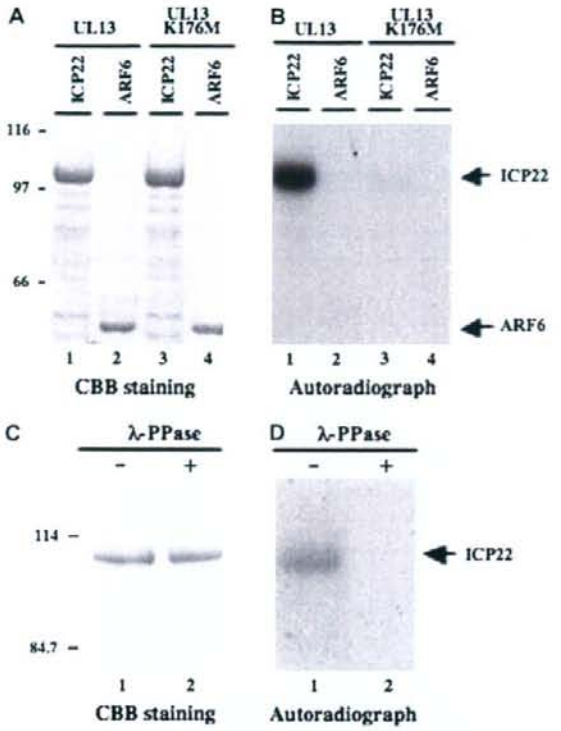


Fig. 2. Autoradiographs of *in vitro* ICP22 phosphorylation. (A) CBB stained images of phosphorylated ICP22. Purified MBP-ICP22 (lanes 1 and 3) and MBP-ARF6 (lanes 2 and 4) were incubated in kinase buffer containing [$\gamma$-$^{32}$P]ATP and purified GST-UL13 (lanes 1 and 2) or GST-UL13K176M (lanes 3 and 4), separated on a denaturing gel, and stained with CBB. Molecular masses (kDa) are shown on the left. (B) Autoradiograph of the gel in panel A. (C) Purified MBP-ICP22 was incubated in kinase buffer containing [$\gamma$-$^{32}$P]ATP and purified GST-UL13 and then either mock-treated (lane 1) or treated with λ-PPase (lane 2), separated on a denaturing gel, and stained with CBB. (D) Autoradiograph of the gel in panel C.

### 3.2. Identification of UL41 as a novel substrate of UL13

To identify novel viral substrate(s) for UL13, several HSV-1 proteins fused to MBP were expressed in *E. coli* and purified, and the purified MBP fusion proteins were subjected to in vitro kinase assay (data not shown). Among the viral proteins tested, we obtained evidence that UL41 is an in vitro substrate of UL13. This conclusion is supported by the following observations. UL41 is a virion component that mediates indiscriminate degradation of mRNA, subsequently causing shuttoff of protein synthesis in infected cells. As shown in Fig. 4C, in the reaction with purified GST-UL13, MBP-UL41, MBP-UL41N and MBP-UL41-C were labeled with [$\gamma$-$^{32}$P]ATP, but MBP-ARF6 was not. When the GST-UL13K176M kinase-negative mutant was used instead of GST-UL13, none of the MBP fusion proteins were labeled. Labeling of MBP-UL41N and MBP-UL41C by GST-UL13 was eliminated by phosphatase treatment (Fig. 4E). The expression of each MBP fusion protein and the identification of each MBP protein-radiolabeled band were

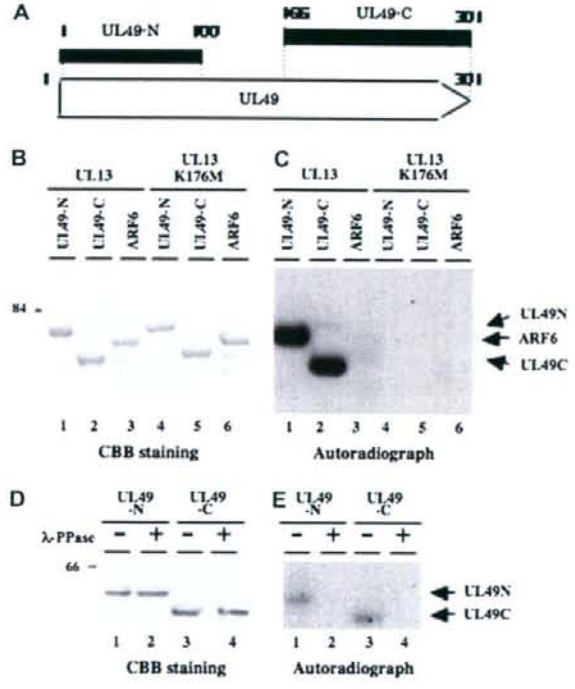


Fig. 3. Autoradiographs of *in vitro* UL49 phosphorylation. (A) Schematic diagram of structures of the UL49 open reading frame. The domains of the UL49 gene used in these studies to generate MBP-UL49 fusion proteins are indicated. (B) CBB stained images of phosphorylated UL49. Purified MBP-UL49N (lanes 1 and 4), MBP-UL49C (lanes 2 and 5), and MBP-ARF6 (lanes 3 and 6) were incubated in kinase buffer containing [$\gamma$-$^{32}$P]ATP and purified GST-UL13 (lanes 1–3) or GST-UL13K176M (lanes 4–6), separated on a denaturing gel, and stained with CBB. Molecular masses (kDa) are shown on the left. (C) Autoradiograph of the gel in panel B. (D) Purified MBP-UL49N (lanes 1 and 2) and MBP-UL49C (lanes 3 and 4) were incubated in kinase buffer containing [$\gamma$-$^{32}$P]ATP and purified GST-UL13 and then either mock-treated (lanes 1 and 3) or treated with λ-PPase (lanes 2 and 4), separated on a denaturing gel, and stained with CBB. (E) Autoradiograph of the gel in panel D.

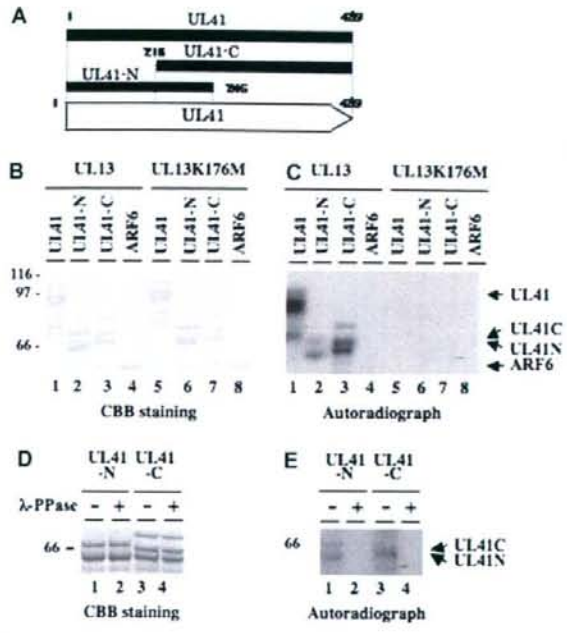


Fig. 4. Autoradiographs of *in vitro* UL41 phosphorylation. (A) Schematic diagram of structures of the UL41 open reading frame. The domains of the UL41 gene used in these studies to generate MBP-UL41 fusion proteins are indicated. (B) CBB stained images of phosphorylated UL41. Purified MBP-UL41 (lanes 1 and 5), MBP-UL49N (lanes 2 and 6), MBP-UL49C (lanes 3 and 7) and MBP-ARF6 (lanes 4 and 8) were incubated in kinase buffer containing [$\gamma$-$^{32}$P]ATP and purified GST-UL13 (lanes 1–4) or GST-UL13K176M (lanes 5–8), separated on a denaturing gel, and stained with CBB. Molecular masses (kDa) are shown on the left. (C) Autoradiograph of the gel in panel B. (D) Purified MBP-UL41N (lanes 1 and 2) and MBP-UL41C (lanes 3 and 4) were incubated in kinase buffer containing [$\gamma$-$^{32}$P]ATP and purified GST-UL13 and then either mock-treated (lanes 1 and 3) or treated with λ-PPase (lanes 2 and 4), separated on a denaturing gel, and stained with CBB. (E) Autoradiograph of the gel in panel D.

verified by CBB staining as shown in Fig. 4B,D. These results show that UL13 directly phosphorylates UL41 *in vitro*.

## 4. Discussion

Identification of the substrates of a protein kinase is the first step to clarify the mechanisms by which the protein kinase functions. Once a substrate has been determined, the phosphorylation site(s) of the substrate can be identified by mass spectrometric analysis or mutational analysis, and the biological significance of phosphorylation can be investigated using substrate mutants with amino acid substitution(s) in the phosphorylation site(s). Identification of UL13 substrates has long been hampered by the difficulty of directly demonstrating specific protein kinase activity *in vitro* [24]. For instance, ICP22 was identified as the first putative substrate of UL13 more than a decade ago [15], based on the observation that the phosphorylation and posttranslational processing of ICP22 is obviated in cells infected with UL13 mutant viruses. However, no studies have so far demonstrated that UL13 directly phosphorylates ICP22 *in vitro*. Our specially developed system to analyze the specific protein kinase activity of UL13 [16] enables us to identify specific UL13 substrates *in vitro*. In the present study, we add to the base knowledge of UL13 substrates and show that previously reported putative substrates of UL13 (ICP22 and UL49) are phosphorylated directly by UL13. Furthermore, our present studies identified UL41, a previously unreported UL13 substrate, as a novel substrate *in vitro*.

Although demonstration that protein substrates are phosphorylated directly by UL13 *in vitro* is important, the protein identified in the present study does not fulfill the requirements to be a natural substrate of UL13 in infected cells. Identification of physiological substrates of a viral protein kinase requires demonstration that the substrate is specifically and directly phosphorylated by the enzyme *in vitro*, and that phosphorylation of the substrate is altered in cells infected with a mutant virus lacking protein kinase activity. We previously identified EF-1δ and Us3 as natural substrates of UL13 that fulfill both of the requirements described above [6,16]. Of the proteins identified to

be phosphorylated directly by UL13 in this study, ICP22 and UL49 have reduced phosphorylation or posttranslational processing in cells infected with UL13 kinase-negative mutant viruses [9,15]. It is therefore likely that ICP22 and UL49 are physiological substrates of UL13 in infected cells. Since phosphorylation of UL41 has not been analyzed thus far in UL13 kinase-negative mutant virus-infected cells, it is not clear at present whether UL41 is a natural substrate of UL13. However, we may speculate that the phosphorylation of UL41 by UL13 regulates the functions of UL41 [25] such as degradation of host mRNAs and the shutoff of host protein synthesis [26] and contributes the optimal viral replication.

In conclusion, we have identified several viral and cellular proteins that are phosphorylated directly by UL13. Taken together with previous reports, some of the identified proteins including ICP22 and UL49 are likely to be physiological substrates of UL13 in infected cells. However, the biological significance of the UL13-mediated phosphorylation of the identified proteins remains unknown. Further studies to resolve this issue are of importance and presently under way in our laboratory. Such studies include the demonstration of altered UL41 phosphorylation in cells infected with UL13 mutant viruses, identification of phosphorylation sites of the UL13 substrates, and investigations of phenotypes of substrate mutants by amino acid substitution(s) in the phosphorylation site(s).

## Acknowledgments

We thank Dr. B. Roizman for pBC1007. We thank S. Koyama for technical assistance. This study was supported in part by Grants-in-Aid for Scientific Research and Grants-in-Aid for Scientific Research in Priority Areas from the Ministry of Education, Culture, Science, Sports and Technology (MEXT) of Japan and Japan Society for the Promotion of Science (JSPS).

## References

[1] R.J. Whitley, Herpes simplex viruses, in: D.M. Knipe, P.M. Howley, D.E. Griffin, R.A. Lamb, M.A. Martin, B. Roizman, S.E. Straus (Eds.), Fields virology, 4th ed. Lippincott-Williams &Wilkins, Philadelphia, PA, 2001, pp. 2461–2509.

[2] A.M. Edelman, D.K. Blumenthal, E.G. Krebs, Protein serine/threonine kinases, Annu. Rev. Biochem. 56 (1987) 567–613.

[3] G. Manning, D.B. Whyte, R. Martinez, T. Hunter, S. Sudarsanam, The protein kinase complement of the human genome, Science 298 (2002) 1912–1934.

[4] F.C. Purves, W.O. Ogle, B. Roizman, Processing of the herpes simplex virus regulatory protein alpha 22 mediated by the UL13 protein kinase determines the accumulation of a subset of alpha and gamma mRNAs and proteins in infected cells, Proc. Natl. Acad. Sci. U. S. A. 90 (1993) 6701–6705.

[5] R. Leopardi, C. Van Sant, B. Roizman, The herpes simplex virus 1 protein kinase US3 is required for protection from apoptosis induced by the virus, Proc. Natl. Acad. Sci. U. S. A. 94 (1997) 7891–7896.

[6] D. Perkins, E.F. Pereira, M. Gober, P.J. Yarowsky, L. Aurelian, The herpes simplex virus type 2 R1 protein kinase (ICP10 PK) blocks apoptosis in hippocampal neurons, involving activation of the MEK/MAPK survival pathway, J. Virol. 76 (2002) 1435–1449.

[7] A.E. Reynolds, E.G. Wills, R.J. Roller, B.J. Ryckman, J.D. Baines, Ultrastructural localization of the herpes simplex virus type 1 UL31, UL34, and US3 proteins suggests specific roles in primary envelopment and egress of nucleocapsids, J. Virol. 76 (2002) 8939–8952.

[8] R. Bruni, B. Fineschi, W.O. Ogle, B. Roizman, A novel cellular protein, p60, interacting with both herpes simplex virus 1 regulatory proteins ICP22 and ICP0 is modified in a cell-type-specific manner and is recruited to the nucleus after infection, J. Virol. 73 (1999) 3810–3817.

[9] L.J. Coulter, H.W. Moss, J. Lang, D.J. McGeoch, A mutant of herpes simplex virus type 1 in which the UL13 protein kinase gene is disrupted, J. Gen. Virol. 74 (1993) 387–395.

[10] L.O. Durand, S.J. Advani, A.P. Poon, B. Roizman, The carboxyl-terminal domain of RNA polymerase II is phosphorylated by a complex containing cdk9 and infected-cell protein 22 of herpes simplex virus 1, J. Virol. 79 (2005) 6757–6762.

[11] Y. Kawaguchi, C. Van Sant, B. Roizman, Eukaryotic elongation factor 1delta is hyperphosphorylated by the protein kinase encoded by the U(L)13 gene of herpes simplex virus 1, J. Virol. 72 (1998) 1731–1736.

[12] M.C. Long, V. Leong, P.A. Schaffer, C.A. Spencer, S.A. Rice, ICP22 and the UL13 protein kinase are both required for herpes simplex virus-induced modification of the large subunit of RNA polymerase II, J. Virol. 73 (1999) 5593–5604.

[13] T.I. Ng, W.O. Ogle, B. Roizman, UL13 protein kinase of herpes simplex virus 1 complexes with glycoprotein E and mediates the phosphorylation of the viral Fc receptor: glycoproteins E and I, Virology 241 (1998) 37–48.

[14] W.O. Ogle, T.I. Ng, K.L. Carter, B. Roizman, The UL13 protein kinase and the infected cell type are determinants of posttranslational modification of ICP0, Virology 235 (1997) 406–413.

[15] F.C. Purves, B. Roizman, The UL13 gene of herpes simplex virus 1 encodes the functions for posttranslational processing associated with phosphorylation of the regulatory protein alpha 22, Proc. Natl. Acad. Sci. U. S. A. 89 (1992) 7310–7314.

[16] Y. Kawaguchi, K. Kato, M. Tanaka, M. Kanamori, Y. Nishiyama, Y. Yamanashi, Conserved protein kinases encoded by herpesviruses and cellular protein kinase cdc2 target the same phosphorylation site in eukaryotic elongation factor 1delta, J. Virol. 77 (2003) 2359–2368.

[17] A. Kato, M. Yamamoto, T. Ohno, H. Kodaira, Y. Nishiyama, Y. Kawaguchi, Identification of proteins phosphorylated directly by the Us3 protein kinase encoded by herpes simplex virus 1, J. Virol. 79 (2005) 9325–9331.

[18] R. Asai, A. Kato, K. Kato, M. Kanamori-Koyama, K. Sugimoto, T. Sairenji, Y. Nishiyama, Y. Kawaguchi, Epstein–Barr virus protein kinase BGLF4 is a virion tegument protein that dissociates from virions in a phosphorylation-dependent process and phosphorylates the viral immediate-early protein BZLF1, J. Virol. 80 (2006) 5125–5134.

[19] Y. Kawaguchi, C. Van Sant, B. Roizman, Herpes simplex virus 1 alpha regulatory protein ICP0 interacts with and stabilizes the cell cycle regulator cyclin D3, J. Virol. 71 (1997) 7328–7336.

[20] M.M. Cavenagh, J.A. Whitney, K. Carroll, C. Zhang, A.L. Boman, A.G. Rosenwald, I. Mellman, R.A. Kahn, Intracellular distribution of Arf proteins in mammalian cells. Arf6 is uniquely localized to the plasma membrane, J. Biol. Chem. 271 (1996) 21767–21774.

[21] P.J. Peters, V.W. Hsu, C.E. Ooi, D. Finazzi, S.B. Teal, V. Oorschot, J.G. Donaldson, R.D. Klausner, Overexpression of wild-type and mutant ARF1 and ARF6: distinct perturbations of nonoverlapping membrane compartments, J. Cell. Biol. 128 (1995) 1003–1017.

[22] H. Radhakrishna, J.G. Donaldson, ADP-ribosylation factor 6 regulates a novel plasma membrane recycling pathway, J. Cell. Biol. 139 (1997) 49–61.

[23] O.A. Jovanovic, F.D. Brown, J.G. Donaldson, An effector domain mutant of Arf6 implicates phospholipase D in endosomal membrane recycling, Mol. Biol. Cell. 17 (2006) 327–335.

[24] T.I. Ng, C. Talarico, T.C. Burnette, K. Biron, B. Roizman, Partial substitution of the functions of the herpes simplex virus 1 U(L)13 gene by the human cytomegalovirus U(L)97 gene, Virology 225 (1996) 347–358.

[25] M. Tanaka, Y. Nishiyama, T. Sata, Y. Kawaguchi, The role of protein kinase activity expressed by the UL13 gene of herpes simplex virus 1: the activity is not essential for optimal expression of UL41 and ICP0, Virology 341 (2005) 301–312.

[26] G.S. Read, B.M. Karr, K. Knight, Isolation of a herpes simplex virus type 1 mutant with a deletion in the virion host shutoff gene and identification of multiple forms of the vhs (UL41) polypeptide, J. Virol. 67 (1993) 7149–7160.

# Loss of smooth muscle calponin results in impaired blood vessel maturation in the tumor–host microenvironment

Hisako Yamamura,[1] Noriko Hirano,[1] Hidenori Koyama,[2] Yoshiki Nishizawa[2] and Katsuhito Takahashi[1,3]

[1]Department of Molecular Medicine and Pathophysiology, Osaka Medical Center for Cancer and Cardiovascular Diseases, Graduate School of Pharmaceutical Science, Osaka University, Osaka City, Osaka 537-8511; [2]Department of Metabolism, Endocrinology, and Molecular Medicine, Osaka City University Graduate School of Medicine, Osaka City, Osaka 545-8585, Japan

(Received November 26, 2006/Revised December 25, 2006/Accepted December 26, 2006/Online publication March 19, 2007)

**The interactions between malignant cells and the microenvironment of the local host tissue play a critical role in tumor growth, metastasis and their response to treatment modalities. We investigated the roles of smooth muscle calponin (*Cnn1*, also called calponin h1 or basic calponin) in the development of tumor vasculature *in vivo* by analyzing mutant mice lacking the *Cnn1* gene. Here we show that loss of *Cnn1* in host mural cells prevents maturation of tumor vasculature. *In vitro* studies showed that platelet-derived growth factor B-induced vascular smooth muscle migration was downregulated by the *Cnn1*-deficiency, and forced expression of *Cnn1* restored migration. Moreover, destruction of established tumor mass by treatment with an antivascular endothelial growth factor antibody was markedly enhanced in *Cnn1*-deficient mice. These data, coupled with the knowledge that structural fragility of normal blood vessels is caused by loss of the *Cnn1* gene, suggest that *Cnn1* plays an important role in the maturation of blood vessels, and may have implications for therapeutic strategies targeting tumor vasculature for treatment of human cancers. (*Cancer Sci* 2007; 98: 757–763)**

Smooth muscle calponin (*Cnn1*) is an actin-associated protein originally isolated from vascular smooth muscle,[1] and is a major regulator of force production in smooth muscle cells (SMC).[2–4] It is generally agreed that *Cnn1* expression serves as an excellent marker for defining lineage specification, differentiation and phenotypic modulation of SMC.[5–7] In previous studies on human cancers, we and others have reported positive and negative expression of *Cnn1* in the mural SMC of tumor vasculature,[8–10] and showed that reduced expression of *Cnn1* in the tumor vasculature of patients with the early stage of hepatocellular carcinoma,[8] and those with renal cell carcinoma,[10] was statistically correlated with poor prognosis. Furthermore, a 17-gene signature set was identified in the tumor–host microenvironment to predict metastatic potential and early death for a variety of human solid tumors.[11] These include decreased expression of the smooth muscle genes γ2 actin (*Actg2*), myosin heavy chain 11 (*MYH11*) and *Cnn1*. However, as yet there is no explanation for links between tumor phenotypes and the observed downregulation of the *Cnn1* gene in host cells, including vascular cells. Although a critical role of the calponin gene in the development of normal vasculature has recently been reported in zebrafish,[12] the role of *Cnn1* in the development and maturation of mammalian blood vessels, especially the tumor vasculature, has not been studied.

## Materials and Methods

**Cells, animals and antibodies.** Lewis lung carcinoma cell line (LLC) was purchased from Riken Cell Bank (RCB0558; Tsukuba, Japan). B16 melanoma cells with low metastatic activity to the lung were kindly provided by Dr H. Tanaka (Osaka Medical Center, Osaka, Japan). *Cnn1*-deficient mice,[13] with a genetic background of C57BL6/J (*Cnn1*$^{-/-}$), were generated through back-crossing to C57BL6/J mice (Nihon SLC, Hamamatsu, Japan) for more than 15 generations. Immunoblot analysis was carried out as described previously.[13] Animal procedures were approved by the Animal Care and Use Committee of Osaka Medical Center.

**Antibodies and immunohistochemistry.** A polyclonal antibody specific to the *Cnn1* isoform was prepared as described previously.[13] Anti-smooth muscle α-actin (α-SMA) (clone 1A4) was purchased from Sigma Chemicals (St Louis, MO, USA). Anti-PECAM-1(CD31) (clone MEC13.3) was from BD PharMingen (San Diego, CA, USA). Anti-PDGFRβ (sc-6252, A-3) was from Santa Cruz Biotechnology (Santa Cruz, CA, USA). Anti-mouse CD34 (clone MEC14.7) was from Hycult Biotechnology (Uden, the Netherland). Anti-NG2 was from Chemicon International (Temacula, CA, USA).

The specimens were fixed in Bouin's solution (15% [v/v] saturated picric acid solution, 1.65% [v/v] formalin and 1% [v/v] acetic acid/phosphate-buffered saline [PBS]) or 10% formaldehyde/PBS and embedded in paraffin. Antigen retrieval was carried out using an autoclave at 121°C for 10 min in a 10-mM citrate buffer (pH 7.0) (*Cnn1*, α-SMA, CD34 and NG2). The procedures described previously[8,13] are available from the authors on request. For staining of CD31, excised tumor specimens were mounted in OCT compound (Miles, Elkhart, USA) and then frozen using liquid nitrogen.

**Quantification of the vasculature.** Individual microvessel counts, as revealed by CD31 or CD34 expression in the endothelium, were carried out using ×400 fields by two independent investigators after assessing for uniformity of staining at low-power fields (×100). Vessel density is expressed as the number of vessel profiles per mm$^2$. In accordance with other published studies,[14,15] the fraction of blood vessels found to be associated with α-SMA-positive cells in more than 50% of the vessel perimeter was defined as the pericyte coverage index. The extent of pericyte coverage on vessels was determined on 15 properly cross-sectioned vessels in each specimen by measuring the proportion of CD31- or CD34-positive vessel perimeter covered by α-SMA-immunoreactive cells. Thirty fields per section and at least two tissue sections were counted.

**Diffusion chamber model of angiogenesis.** LLC cells ($4 \times 10^7$/mL cells in 200 μL of serum-free Dulbecco's modified Eagle's medium [DMEM]) were injected into the diffusion chamber ring (PR00-014-00; Millipore, Bedford, MA, USA), and the

[3]To whom correspondence should be addressed.
E-mail: takahasi-ka@mc.pref.osaka.jp
The authors declare that they have no competing financial interests.

doi: 10.1111/j.1349-7006.2007.00452.x

chamber was inserted into the skin fold on the back of 6-week-old BALB/c athymic nude mice. Tissues containing angiogenic vasculature were excised 6 days after the implantation, fixed in Bouin's solution, sectioned and immunostained with the anti-*Cnn1* antibody.

**Preparation of primary cultured vascular smooth muscle cells.** Aortas from 4-week-old wild-type and *Cnn1*$^{-/-}$ mice were minced and incubated for 2 h at 37°C in 1.0 mg/mL collagenase (Worthington Biochemicals, Lakewood, NJ, USA), 0.375 mg/mL soybean trypsin inhibitor (Worthington Biochemicals), 0.125 mg/mL elastase III (Sigma Chemicals) and 2 mg/mL bovine serum albumin (BSA) in HEPES buffer (pH 7.5). Cells were washed, cultured in DMEM containing 10% FCS and characterized by spindle-shaped morphology and immunostaining for α-SMA.

**Migration assay and construction of adenovirus vectors.** Migration was assayed in a 48-well chamber (Nucleopore, Bethesda, MD, USA) with a polycarbonate filter (PVP free, 8 μm pores) coated with 300 μg/mL type I collagen. SMC ($1 \times 10^4$ per well) were added to the top wells of the chamber in DMEM containing 0.25% BSA. The bottom wells were filled with DMEM containing 10 ng/mL recombinant platelet-derived growth factor (PDGF)-B/B (Gibco BRL, Carlsbad, CA, USA). The chambers were then incubated for 4 h at 37°C in a humidified atmosphere with 5% $CO_2$. The filters were fixed and stained with Diff-Quik (Kokusai Shiyaku, Kobe, Japan), and migrated cells were counted. Recombinant adenovirus (Ad) vectors expressing *Escherichia coli LacZ* or human *Cnn1* were generated using unique *I-Ceu*I and *PI-Sce*I sites in the E1 deletion region.[16] Ad-*Cnn1* and Ad-*LacZ* were prepared by transfection to human embryonic kidney 293 cells.

***In vivo* treatment of vascular endothelial growth factor (VEGF)-neutralizing antibody.** LLC cells ($1 \times 10^7$/mL in 50 μL PBS) were injected subcutaneously into 6-week-old male wild-type and *Cnn1*$^{-/-}$ mice ($n = 8$ each), and tumor size was monitored. At 10 days after injection, the 'VEGF ablation' groups ($n = 4$) were treated with 8 μg per mouse of goat antimouse VEGF-neutralizing antibody (AF-493-NA; R&D Systems, Minneapolis, MN, USA) administered intraperitoneally every 72 h. Control groups ($n = 4$) were treated with 8 μg per mouse of non-immune goat IgG. Treatment was stopped after a total of four injections.

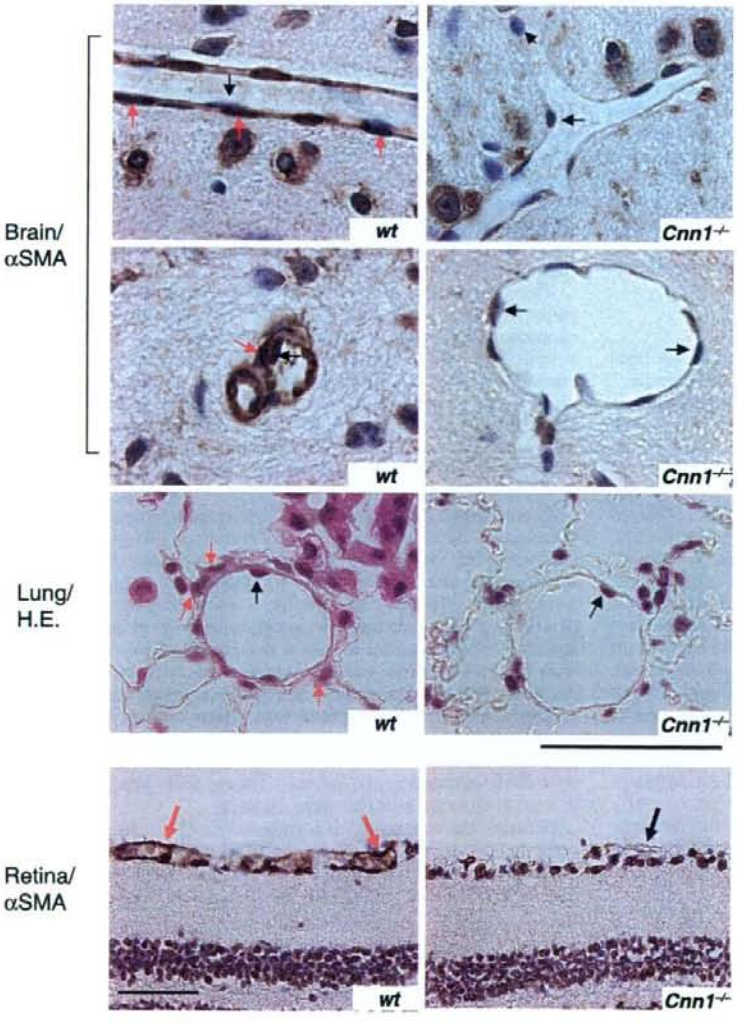


**Fig. 1.** Impaired maturation of blood vessels in normal tissues in smooth muscle calponin-deficient (*Cnn1*)$^{-/-}$ mice. Capillaries in brain (smooth muscle α-actin [α-SMA] immunostaining), lung (hematoxylin–eosin [H&E] staining) and retina (α-SMA immunostaining) in *Cnn1*$^{-/-}$ mice showed loss of pericytes/smooth muscle cells (SMC) (red arrows) attachment to the endothelium (black arrows). Note the dilation of the *Cnn1*$^{-/-}$ capillary in brain. Scale bar = 50 μm in brain and lung, or 100 μm in retina.



doi: 10.1111/j.1349-7006.2007.00452.x

***In situ* apoptosis detection.** Apoptosis was detected by the modified terminal deoxynucleotidyl transferase-mediated deoxyuridine triphosphate-biotin nick-end labeling (TUNEL) method, using an *In Situ* Apoptosis Detection Kit (Takara Biomedicals, Tokyo, Japan) according to the manufacturer's methods.

**Statistical analysis.** Statistical differences were determined using the unpaired Student's *t*-test. Differences were considered statistically significant at $P < 0.05$.

## Results and Discussion

Microvessels in the brain cortex, lung sections and retina from 6-week-old *Cnn1*$^{-/-}$ mice were found to have thinner walls with fewer mural cell layers than those from wild-type mice. Enlarged and naked endothelial tubes were scored in 16/132 cases in wild-type brain sections ($n = 3$) and in 166/218 cases in *Cnn1*$^{-/-}$ brain sections ($n = 5$). Representative examples from the α-SMA- or hematoxylin–eosin (H&E) staining of the brain, lung and retina sections are shown in Fig. 1. Reduced numbers of α-SMA-positive mural cells in *Cnn1*$^{-/-}$ mice were demonstrated in the immunohistochemistry of the brain and retina sections (Fig. 1). These findings are reminiscent of the impaired recruitment of pericytes to brain capillaries in mice lacking PDGF-B[17] or PDGF receptor (R)-β,[18] and are consistent with ultrastructural studies on the microvessels in the ocular fundus, lung and heart of *Cnn1*$^{-/-}$ mice, demonstrating reduced mural SMC layers and increased leakiness.[19]

LLC transplants were established in syngeneic wild-type and *Cnn1*$^{-/-}$ mice. Compared with wild-type mice, the primary tumor growth was reduced in *Cnn1*$^{-/-}$ mice (Fig. 2a). Counting the CD31- or CD34-immunoreactive microvessels in vascular hot spots of LLC (microvessel density; MVD) revealed that there was a significant decrease in the MVD of tumors in *Cnn1*$^{-/-}$ mice compared with those in wild-type mice at 28 days of tumor transplantation (Fig. 2b). The decrease in MVD in *Cnn1*$^{-/-}$ mice was also observed in the size-matched tumors (approximately 600 mm$^3$) (Fig. 2b). To quantitatively assess the maturation status of the tumor vasculature, the number of microvessels covered by α-SMA-immunoreactive mural cells (pericytes or SMC) was determined for LLC at 12 and 28 days after transplantation. There was a striking difference in the percentage of capillaries associated with α-SMA-positive mural cells (MCI; mural cell-coverage index) between wild-type and *Cnn1*$^{-/-}$ tumor blood vessels at 28 days, with no difference at 12 days when the vasculatures were immature (Fig. 2c). In contrast to the wild-type mice, most capillaries in *Cnn1*$^{-/-}$ mice were enlarged (Fig. 2c), distorted and partially enveloped in less than 50% of the vessel surface by cells with α-SMA immunoreactivities. Blood vessels within B16 melanoma tumors generated in *Cnn1*$^{-/-}$ mice also showed reduced mural cell coverage and increased vascular diameter compared with those in wild-type mice (Fig. 2d). Immunohistochemical analysis using antibodies against CD34, α-SMA and a pericyte marker NG2 showed reduced mural cell coverage in the representative blood vessels in both the LLC and B16 melanoma xenografts in *Cnn1*$^{-/-}$ mice (Fig. 2e). Collectively, abnormalities in the morphology of tumor vasculature as well as the phenotype of normal vessels in brain and lung tissues by *Cnn1* deletion were characterized by reduced mural cell association with endothelium, indicating impaired maturation of blood vessels.[20]

Analysis of anti-α-SMA-immunostained (Fig. 3a) and anti-CD34-immunostained (data not shown) vessels in LLC tumors revealed that reduction of the MCI in the vasculature of *Cnn1*$^{-/-}$ mice was observed predominantly in the central region of tumors but not at the periphery or in the extra-tumor connective

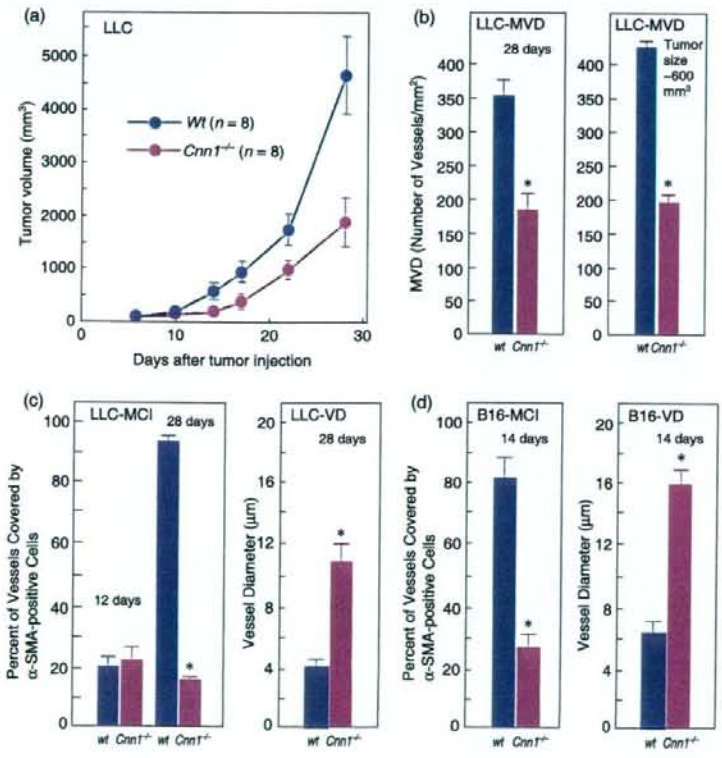


**Fig. 2.** Impaired maturation of blood vessels in tumor tissues in smooth muscle calponin-deficient (*Cnn1*)$^{-/-}$ mice. (a) Primary tumor growth of Lewis lung carcinoma (LLC) xenografts implanted into the flank ($5 \times 10^5$ cells/mouse) was significantly reduced in *Cnn1*$^{-/-}$ mice. (b–d) Immunohistochemical analysis (CD31 or CD34, smooth muscle α-actin [α-SMA] and NG2) showed reduced microvessel densities (MVD) (b) and fraction of vessels with mural cell-coverage (MCI) of tumor blood vessels of LLC ($n = 4$) at 28 days after implantation and B16 melanoma ($5 \times 10^5$ cells/mouse) ($n = 4$) at 14 days after implantation (c,d). The decrease in MVD in *Cnn1*$^{-/-}$ mice was also observed in the size-matched LLC tumors (approximately 600 mm$^3$). Blood vessels in both tumors also showed enlarged diameter (c,d). (e) Representative tumor vessels in wild-type and *Cnn1*$^{-/-}$ mice showed reduced MVD and MCI. Arrows indicate endothelial cells (black) and smooth muscle cells (SMC) (red). Scale bars = 50 μm. The data are mean ± SE (30 high-power field analyses per group). *$P < 0.05$.

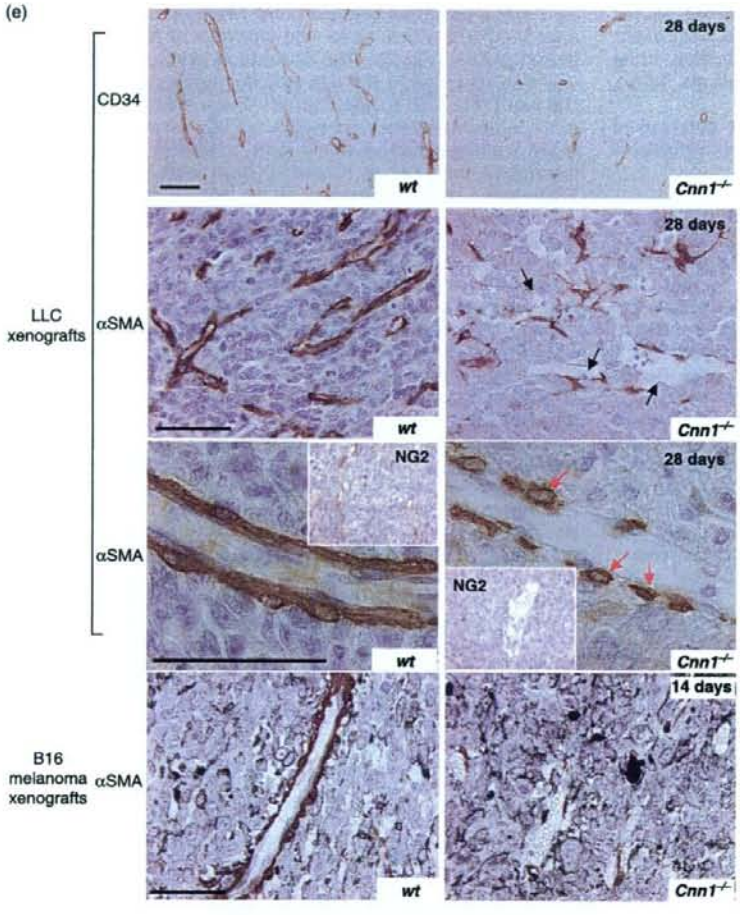


Fig. 2. *Continuet*

tissue (Fig. 3a,b). During the tumor-induced angiogenesis, *Cnn1* was normally expressed by peri-endothelial cells, most probably pericytes or SMC (Fig. 3c), as those *Cnn1*-positive cells were also positive for α-SMA (data not shown). Some of the *Cnn1*-positive cells in newly formed vasculature in both mouse (not shown) and human tumors (Fig. 3c) were proliferating. Previous studies suggest that for recruitment of the mural cells to angiogenic vasculature, their migration to the endothelium via PDGF-B and PDGFR-β signaling is functionally important.[17,18,20] *Cnn1* is involved in the force generation of actin and myosin in SMC.[2–4] We therefore investigated the effects of *Cnn1* deletion on PDGF-B-induced migration of vascular SMC *in vitro*, using the Boyden chamber analysis. As illustrated in Fig. 3d, both wild-type and $Cnn1^{-/-}$ SMC cultured from aorta were found to express PDGFR-β polypeptides, whereas only wild-type SMC expressed *Cnn1*. We also prepared $Cnn1^{-/-}$ SMC lines reconstituted with full-length *Cnn1* by adenovirus-mediated gene transfer (Fig. 3d). Analysis of migration revealed that approximately 45% less $Cnn1^{-/-}$ SMC than wild-type SMC migrated through a porous membrane coated with type I collagen in response to a gradient of PDGF-B, and also in its absence (Fig. 3e). Reconstitution of *Cnn1* expression by adenovirus reversed the inhibition of PDGF-B-induced migration of $Cnn1^{-/-}$ SMC up to levels that corresponded to wild-type SMC, whereas the inhibition of basal migration was not reversed. Thus, *Cnn1* deletion results in reduced chemotactic migration of SMC to PDGF-B.

Given the reduced mural cell association, implicating immaturity of blood vessels, it is likely that $Cnn1^{-/-}$ tumor vessels display VEGF-dependent remodeling of capillary structures, and endothelial and cancer cell survival.[21,22] We therefore tested whether the tumor vasculature in $Cnn1^{-/-}$ mice is sensitized to anti-angiogenesis treatment targeting VEGF. Implanted LLC cells in wild-type and $Cnn1^{-/-}$ mice were allowed to grow for 10 days, forming flank tumors ($n = 8$ each). Animals in the wild-type and $Cnn1^{-/-}$ groups were divided randomly and injections of mouse VEGF-specific neutralizing antibody or normal goat IgG were then given intraperitoneally twice a week for 2 weeks. Strikingly, at 18 days after initial anti-VEGF antibody injection, the treated tumors in $Cnn1^{-/-}$ mice were found to have prominent degeneration when compared with those in wild-type mice. Representative examples from macroscopic examination of the H&E-stained sections of the treated and untreated tumors are shown in Fig. 4a. It depicts extensive necrosis, vulnerability of immature vessels with hemorrhage, and more prominent obliteration of tumor vasculature in $Cnn1^{-/-}$ mice than in wild-type mice (Fig. 4b). An *in situ* apoptosis analysis (TUNEL) revealed that TUNEL-positive endothelial cells and cancer cells were rarely detected in untreated tumors in wild-type mice. In contrast, cancer cells transplanted in $Cnn1^{-/-}$ mice, even in untreated tumors, displayed significant propensity of apoptosis (Fig. 4c). In addition, the anti-VEGF antibody treatment increased TUNEL-positive endothelial cells more potently in $Cnn1^{-/-}$ mice



doi: 10.1111/j.1349-7006.2007.00452.x

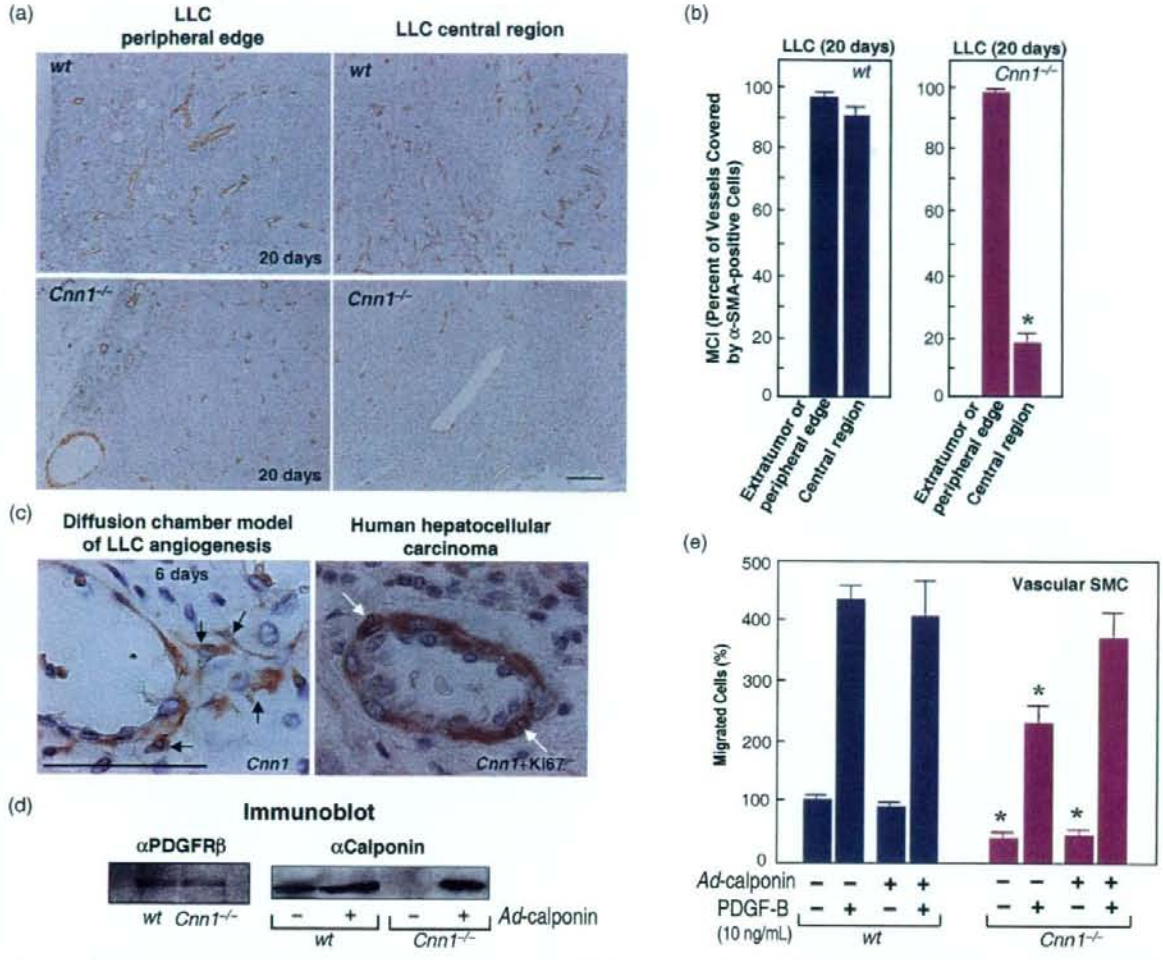


**Fig. 3.** (a,b) Prominent reduction of the mural cell-coverage (MCI) in smooth muscle calponin-deficient (*Cnn1*)$^{-/-}$ mice in the central region of tumors but not at the periphery of tumor tissues. Lewis lung carcinoma (LLC) xenografts were analyzed at 20 days after implantation ($5 \times 10^5$ cells/mouse). Scale bar = 100 μm. (c) *Cnn1* was expressed in mural cells (black arrows) surrounding endothelial cells. Note the double staining of mural cells with *Cnn1* (cytoplasm) and Ki-67 (nucleus), an indicator of proliferating cells (white arrows). Scale bar = 50 μm. (d) Platelet-derived growth factor (PDGF) receptor β was expressed in both wild-type and *Cnn1*$^{-/-}$ mice, whereas *Cnn1* was expressed only in wild-type mice. Add-back of *Cnn1* expression in *Cnn1*$^{-/-}$ smooth muscle cells (SMC) was carried out by adenovirus-mediated transfection (multiplicity of infection = 30) of *Cnn1* cDNA. (e) Reduced SMC migration by *Cnn1* deletion. Inhibition of PDGF-B/B (10 ng/mL)-induced migration was compensated by the reconstitution of *Cnn1*, whereas random migration was not. The experiment was repeated twice, and the data are mean ± SE ($n = 4$ per group). *$P < 0.05$.

than in wild-type mice (data not shown). The anti-VEGF antibody can decrease MVD in both wild-type and *Cnn1*$^{-/-}$ mice (Fig. 4d). The MCI of the tumor vessels in *Cnn1*$^{-/-}$ mice increased significantly after treatment (Fig. 4e), indicating selective destruction of the fraction of vessels negative for α-SMA and normalization of tumor vasculature[23] (Fig. 4f). The results suggest that, under the experimental conditions used, reduced MCI in LLC tumor vasculature in *Cnn1*$^{-/-}$ mice may be caused by VEGF. The relationship between *Cnn1* deficiency and VEGF production in mural cells should be clarified in the future study. Moreover, consistent with the notion that angiogenesis inhibitors control tumor growth by increasing apoptosis of tumor cells, the anti-VEGF antibody was found to be more efficacious in killing pre-existing cancer cells in *Cnn1*$^{-/-}$ mice than in wild-type mice.

Assembly of mural cells to endothelial cells is well known to play a critical role in vessel maturation,[17,18,20–22] and it has been demonstrated that treatments targeted at killing both endothelial and mural cells are more effective in cancer treatment in preclinical animals.[22] Thus, an understanding of the molecular mechanism of mural cell recruitment to tumor endothelial cells is important for cancer treatment. However, genes as well as molecular pathways in mural cells controlling their assembly to the tumor vasculature are not fully understood. The results presented here, for the first time, demonstrate an important role for the *Cnn1* gene in vascular maturation at the tumor–host interface. Recent studies have demonstrated that knockdown of calponin in zebrafish blocks the proper migration of endothelial cells during formation of intersegmental vessels.[12] We now report that loss of *Cnn1* expression in SMC results in reduced chemotactic migration of SMC to PDGF-B, suggesting that it may cause defective SMC coverage of the tumor microvessels in *Cnn1*$^{-/-}$ mice. Our results also demonstrated that the properties of tissue

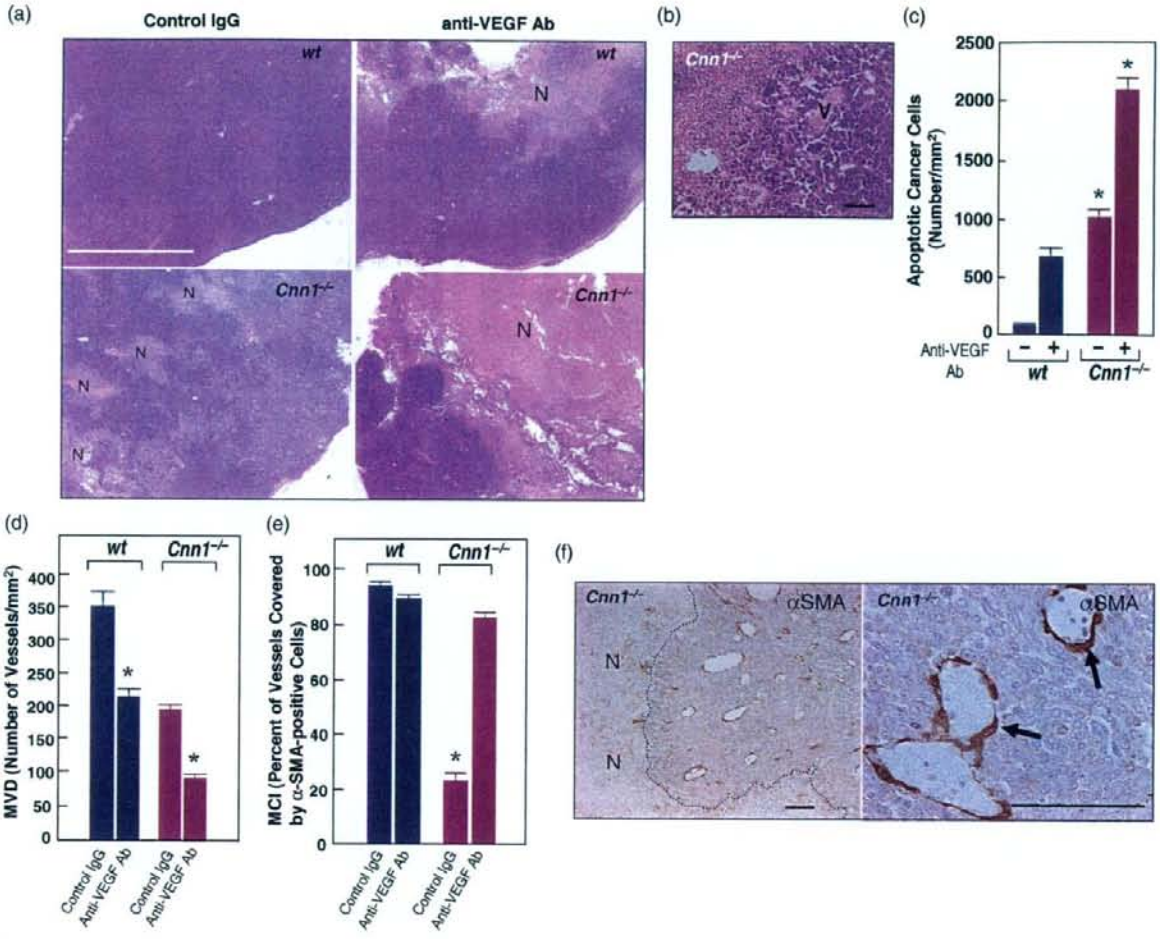


**Fig. 4.** Deletion of smooth muscle calponin (*Cnn1*)$^{-/-}$ leads to sensitization of cancer cells to anti-vascular endothelial growth factor (VEGF) antibody treatment. (a) Macroscopic view of hematoxylin–eosin (H&E)-stained sections of Lewis lung carcinoma (LLC) tumors 18 days after initial anti-angiogenesis therapy showed the most extensive necrosis of cancer cells (N) in anti-VEGF antibody-treated *Cnn1*$^{-/-}$ mice. Note that in *Cnn1*$^{-/-}$ mice, even non-treated tumor showed focal necrosis of cancer cells (N). White bar = 5 mm. (b) Higher magnification pictures show prominent destruction of tumor vasculature (V) in anti-VEGF antibody-treated LLC tumors in *Cnn1*$^{-/-}$ mice. Black bar = 50 μm. (c) Quantitation of TUNEL assay of tissue sections from the tumors in part (a), showing a striking increase in the number of apoptotic cancer cells in anti-VEGF antibody-treated LLC tumors in *Cnn1*$^{-/-}$ mice. Mean ± SE (30 high-power field analyses from four mice). $*P < 0.05$. (d–f) Treatment with anti-VEGF antibody significantly reduced the microvessel densities (MVD) in both wild-type and *Cnn1*$^{-/-}$ mice (d) and normalized the pericyte coverage index (PCI) in *Cnn1*$^{-/-}$ mice (e). Blood vessels covered by smooth muscle α-actin (α-SMA)-positive mural cells in *Cnn1*$^{-/-}$ mice were refractory to the anti-VEGF antibody therapy (f). Scale bar = 100 μm.

vasculature affected by *Cnn1* expression in mural cells play an important role in determining tumor phenotypes such as apoptosis and susceptibility to the treatment modalities.

Based on a current model of vessel assembly and remodeling,[20,21] our results imply that when tumor cells continue to express high levels of VEGF, reduced expression of *Cnn1* in local mural cells may lead to a rapid growth of leaky tumor vessels. Previous studies have demonstrated that when fluorescein is injected intravenously into mice, *Cnn1*$^{-/-}$ mice exhibit a greater and more rapid leakage of fluorecein from the blood vessels of the ocular fundus compared with wild-type mice.[19] These blood vessel phenotypes in *Cnn1*$^{-/-}$ mice may help to promote metastasis of the tumor cells as implicated by identification of *Cnn1* downregulation as a metastasis signature of solid tumors.[11] The *Cnn1*$^{-/-}$ phenotype of the host tissues, in fact, promotes lung metastasis of solid tumors.[19] We suggest that the status of vessel maturation evaluated by *Cnn1* expression in the mural cells of a given tumor may predict the efficacy of anti-angiogenesis treatments aimed at VEGF ablation, currently being used in the clinical stage.[21,22]

The finding that the vessel maturity changes in *Cnn1*$^{-/-}$ mice affect the vasculature in the central region of the tumor more than at the periphery and in the extra-tumor connective tissue raises the intriguing possibility that the effects may instead be due to a response to hypoxia of *Cnn1*$^{-/-}$ SMC at the tumor–host interface.

The results of the present study indicate that there is the potential for development of a new stromal therapy as a strategy for anticancer treatment. For example, viral replication controlled by the *Cnn1* promoter can destroy activated mural cells with *Cnn1* expression while sparing normal quiescent SMC.[24] We envision that, at least for certain human cancers with strong angiogenic capacity, combinatorial use of the viral agent target-



doi: 10.1111/j.1349-7006.2007.00452.x

ing mural cells may potentiate the efficacy of anti-VEGF antibody treatment. Prevention of vessel maturation in expanding tumors by silencing *Cnn1* expression may also be exploited for enforcing vessel regression via VEGF-withdrawal therapy, and may provide clues for solving the prevention of rarefaction of mature vessels that are refractory to VEGF in retinopathy of prematurity.[25]


## Acknowledgments

This work was supported in part by Grants-in-Aids for Scientific Research from the Ministry of Education, Science, Sports and Culture, Japan, the Ministry of Health and Welfare, Japan, the Princes Takamatsu Cancer Research Fund (Tokyo).


## References


1 Takahashi K, Hiwada K, Kokubu T. Vascular smooth muscle calponin: a novel troponin T-like protein. *Hypertension* 1988; **11**: 620–6.
2 Takahashi K, Yamamura H. Studies and perspectives of calponin in smooth muscle regulation and cancer gene therapy. *Adv Biophys* 2003; **37**: 91–111.
3 Matthew JD, Khromov AS, McDuffie MJ *et al.* Contractile properties and proteins of a calponin knockout mouse. *J Physiol (London)* 2000; **529**: 811–24.
4 Babu GJ, Celia G, Rhee AY *et al.* Effects of h1-calponin ablation on the contractile properties of bladder vs vascular smooth muscle in SM-B null mice. *J Physiol (London)* 2006; **577**: 1033–42.
5 Takahashi K, Nadal-Ginard B. Molecular cloning and sequence analysis of smooth muscle calponin. *J Biol Chem* 1991; **266**: 13 284–8.
6 Miano JM, Olsen EN. Expression of the smooth muscle cell calponin gene marks the early cardiac and smooth muscle cell lineages during mouse embryogenesis. *J Biol Chem* 1996; **271**: 7095–103.
7 Yamashita J, Itoh H, Hirashima M *et al.* Flk1-positive cells derived from embryonic stem cells serve as vascular progenitors. *Nature* 2000; **408**: 92–6.
8 Sasaki Y, Yamamura H, Kawakami Y *et al.* Expression of smooth muscle calponin in tumor vessels of human hepatocellular carcinoma and its possible association with prognosis. *Cancer* 2002; **94**: 1777–86.
9 Koganeshita Y, Takeoka M, Ehara T *et al.* Reduced expression of actin-binding proteins, h-caldesmon and calponin h1, in the vascular smooth muscle inside melanoma lesions: an adverse prognostic factor for malignant melanoma. *Br J Dermatol* 2003; **148**: 971–80.
10 Islam AH, Ehara T, Kato H *et al.* Calponin h1 expression in renal tumor vessels: correlation with multiple pathological factors of renal cell carcinoma. *J Urol* 2004; **171**: 1319–23.
11 Ramaswamy S, Ross KN, Lander ES, Golub TR. A molecular signature of metastasis in primary solid tumors. *Nature Genet* 2003; **33**: 49–54.
12 Tang J, Hu G, Hanai J *et al.* A critical role for calponin 2 in vascular development. *J Biol Chem* 2006; **281**: 6664–72.
13 Yoshikawa H, Taniguchi S, Yamamura H *et al.* Mice lacking smooth muscle calponin display increased bone formation that is associated with enhancement of bone morphogenetic protein responses. *Genes Cells* 1998; **3**: 685–95.
14 Eberhard A, Kahlert S, Goede V, Hemmerlein B, Plate KH, Augustin HG. Heterogeneity of angiogenesis and blood vessel maturation in human tumors: implication for antiangiogenic tumor therapies. *Cancer Res* 2000; **60**: 1388–93.
15 Morikawa S, Baluk P, Kaidoh T, Haskell A, Jain RK, McDonald DM. Abnormalities in pericytes on blood vessels and endothelial sprouts in tumors. *Am J Pathol* 2002; **160**: 985–1000.
16 Morioka T, Koyama H, Yamamura H *et al.* Role of h1-calponin in pancreatic AR42J cell differentiation into insulin-producing cells. *Diabetes* 2003; **52**: 760–6.
17 Lindahl P, Johansson BR, Leveen P, Betsholtz C. Pericyte loss and microaneurysm formation in PDGF-B-deficient mice. *Science* 1997; **277**: 242–5.
18 Hellstrom M, Kalen M, Lindahl P, Abramsson A, Betsholtz C. Role of PDGF-B and PDGFR-β in recruitment of vascular smooth muscle cells and pericytes during embryonic blood vessel formation in the mouse. *Development* 1999; **126**: 3047–55.
19 Taniguchi S, Takeoka M, Ehara T *et al.* Structural fragility of blood vessels and peritoneum in calponin h1-deficient mice, resulting in an increase in hematogenous metastasis and peritoneal dissemination of malignant tumor cells. *Cancer Res* 2001; **61**: 7627–34.
20 Jain RK, Booth MF. What brings pericytes to tumor vessels? *J Clin Invest* 2003; **112**: 1134–6.
21 Benjamin LE, Golijanin D, Itin A, Pode D, Keshet E. Selective ablation of immature blood vessels in established human tumors follows vascular endothelial growth factor withdrawal. *J Clin Invest* 1999; **103**: 159–65.
22 Bergers G, Song S, Meyer-Morse N, Bergsland E, Hanahan D. Benefits of targeting both pericytes and endothelial cells in the tumor vasculature with kinase inhibitors. *J Clin Invest* 2003; **111**: 1287–95.
23 Willet CG, Boucher Y, di Tomaso E *et al.* Direct evidence that the VEGF-specific antibody bevacizumab has antivascular effects in human rectal cancer. *Nature Med* 2004; **10**: 145–7.
24 Yamamura H, Hashio M, Noguchi M *et al.* Identification of the transcriptional regulatory sequences of human calponin promoter and their use in targeting a conditionally replicating herpes vector to malignant human soft tissue and bone tumors. *Cancer Res* 2001; **61**: 3969–77.
25 Keshet E. Preventing pathological regression of blood vessels. *J Clin Invest* 2003; **112**: 27–9.

*Journal of General Virology* (2008), **89**, 188–194 DOI 10.1099/vir.0.83208-0

# A silkworm–baculovirus model for assessing the therapeutic effects of antiviral compounds: characterization and application to the isolation of antivirals from traditional medicines

Yutaka Orihara,[1]† Hiroshi Hamamoto,[2]† Hiroshi Kasuga,[3] Toru Shimada,[4] Yasushi Kawaguchi[5] and Kazuhisa Sekimizu[2,3]

**Correspondence**
Kazuhisa Sekimizu
sekimizu@mol.f.u-tokyo.ac.jp

[1]Experimental Station for Medical Plant Studies, Graduate School of Pharmaceutical Sciences, The University of Tokyo, 7-3-1 Hongo, Bunkyo-ku, Tokyo 113-0033, Japan

[2]Genome Pharmaceuticals Institute Co. Ltd, The University of Tokyo Entrepreneur Plaza, 7-3-1 Hongo, Bunkyo-ku, Tokyo 111-0033, Japan

[3]Laboratory of Microbiology, Graduate School of Pharmaceutical Sciences, The University of Tokyo, 7-3-1 Hongo, Bunkyo-ku, Tokyo 113-0033, Japan

[4]Laboratory of Insect Genetics and Bioscience, Department of Agricultural and Environmental Biology, Graduate School of Agricultural and Life Sciences, The University of Tokyo, 1-1-1 Yayoi, Bunkyo-ku, Tokyo 113-8657, Japan

[5]Division of Viral Infection, Department of Infectious Disease Control, International Research Center for Infectious Diseases, The Institute of Medical Science, The University of Tokyo, 4-6-1 Shirokanedai, Minato-ku, Tokyo 108-8639, Japan

Ganciclovir, foscarnet, vidarabine and ribavirin, which are used to treat viral infections in humans, inhibited the proliferation of a baculovirus (*Bombyx mori* nucleopolyhedrovirus) in BmN4 cells, a cultured silkworm cell line. These antiviral agents inhibited the proliferation of baculovirus in silkworm body fluid and had therapeutic effects. Using the silkworm infection model, the antiviral activity of Kampo medicines was screened and it was found that cinnamon bark, a component of the traditional Japanese medicine Mao-to, had a therapeutic effect. Based on the therapeutic activity, the antiviral substance was purified. Nuclear magnetic resonance analysis of the purified fraction revealed that the antiviral activity was due to cinnzeylanine, which has previously been isolated from *Cinnamomum zeylanicum*. Cinnzeylanine inhibits the proliferation of herpes simplex virus type 1 in Vero cells. These results suggest that the silkworm–baculovirus infection model is useful for screening antiviral agents that are effective for treating humans infected with DNA viruses.

Received 2 June 2007
Accepted 19 September 2007

## INTRODUCTION

To develop antiviral agents, compounds that show inhibitory effects on the proliferation of the target virus in cultured mammalian cells are screened in libraries of synthetic compounds and chemicals obtained from natural resources. The therapeutic effects of candidate substances are then examined by using mammalian models. Most compounds selected from *in vitro*-cultured cell systems have no therapeutic effects, because of their pharmacodynamics in host animals. Therefore, a large number of mammalian animals must be killed to collect data in the preclinical stages, which is costly and leads to ethical issues (EU, 1986; Orlans *et al.*, 1998). To overcome these problems, the use of invertebrate animals for evaluating the therapeutic effects of antiviral agents in the early stages of screening has been proposed.

We reported previously that silkworms are a useful animal model of infection from bacteria pathogenic to humans (Hamamoto *et al.*, 2004; Kaito *et al.*, 2002). Silkworms can be cultivated by using artificial food at any time of the year. Furthermore, a large number of silkworms can be produced at low cost. We demonstrated that antibiotics used clinically to treat infected humans are effective in silkworms, and that the $ED_{50}$ values of the antibiotics used in the silkworm infection model are consistent with those obtained in mammalian animal models (Hamamoto *et al.*, 2004, 2005; Hamamoto & Sekimizu, 2005; Kaito *et al.*, 2002, 2005). Silkworms have enzymes, P450s and conjugating enzymes (Hamamoto *et al.*, 2005; Li *et al.*, 2005; Luque *et al.*, 2002) that are involved in metabolizing

†These authors contributed equally to this work.

antibiotics. Silkworms are large enough for antiviral agents to be injected into their midgut and haemolymph by using syringes.

Baculoviruses infect silkworms (Kool *et al.*, 1995; Rohrmann, 1994; Szewczyk *et al.*, 2006). Among the baculoviruses, *Bombyx mori* nucleopolyhedrovirus (BmNPV) is used as a vector for the overproduction of recombinant proteins. Proliferation of *Autographa californica* nucleopolyhedrovirus (AcNPV) in cultured cells is inhibited by ganciclovir, an antiviral agent used clinically to treat infected humans (Ansari & Emery, 1999; Safronetz *et al.*, 2003). The amino acid sequence of BmNPV DNA polymerase has a high similarity (96 %) to that of AcNPV. BmNPV DNA polymerase also has a high similarity, especially with regard to functional domains, to the herpesvirus and cytomegalovirus DNA polymerases. Therefore, it is expected that ganciclovir would inhibit the DNA polymerases of all of these viruses.

In this paper, we describe methods for evaluating, in the silkworm infection model, the therapeutic effects of anti-DNA virus agents that are used clinically to treat human patients. We also demonstrate the purification of antiviral agents in Kampo medicines by using the silkworm infection model.

## METHODS

**Animals and reagents.** Silkworm eggs (Hu·Yo × Tsukuba·Ne) were purchased from Ehime Sansyu and raised until the fourth-instar larval stage, using artificial food (Silkmate 2S; Nosan Corporation). Silkworm larvae were reared as described previously (Hamamoto *et al.*, 2004; Hamamoto & Sekimizu, 2005). Reagent-grade powders of ganciclovir and vidarabine were kindly provided by Tanabe Seiyaku Co. Ltd and Mochida Pharmaceutical Co. Ltd, respectively. Ribavirin and foscarnet were purchased from Duchefa and Alfa Aesar, respectively. Unless otherwise stated, all other reagents were reagent-grade commercial products.

**Evaluation of therapeutic effects of antiviral agents used clinically to treat infected humans and of plant extracts from Kampo medicines in silkworms infected with baculovirus.** Artificial diets were fed to fifth-instar silkworm larvae on the first day for 1 day, and baculovirus (BmNPV FP #128; Katsuma *et al.*, 1999) solution containing $1.6 \times 10^4$ virions in 0.05 ml was injected into the haemolymph by using a disposable syringe (Terumo) with a 27 G needle. Silkworms were raised for 5 days with the artificial diets at 24 °C. When all of the animals in the virus-infection control group, which did not receive medicine, had died, the number of surviving silkworms injected with test samples was counted and the $ED_{50}$ values were calculated.

Vidarabine and ganciclovir were dissolved in 0.9 % NaCl containing 20 % DMSO. Foscarnet and ribavirin were dissolved in 0.9 % NaCl. Each sample (0.05 ml) was injected into the haemolymph of silkworms. Three days after injection, the silkworm haemolymph was harvested and the number of virion particles was estimated by using the plaque-forming method.

Hot-water extracts of Kakkon-to (pueraria root, jujube fruit, ephedra herb, cinnamon bark, licorice root, peony root and ginger rhizoma), Mao-to (ephedra herb, apricot kernel, licorice root and cinnamon bark) and Shosaiko-to (bupleurum root, pinellia tuber, scutellaria root, jujube fruit, ginseng root, licorice root and ginger rhizoma), which are traditional Japanese medicines that are related closely to traditional Chinese medicines, and each individual ingredient of Mao-to were prepared, and 0.5 ml of each sample was injected into the midgut of silkworms. Purified fractions of cinnzeylanine from Mao-to were also injected into the haemolymph of silkworms.

**Baculovirus plaque assay.** BmN cells ($1 \times 10^7$) were suspended in 4 ml TC100 medium (Funakoshi), plated on a tissue-culture dish (60 mm diameter; Asahi Techno Glass Co.) and incubated at 27 °C for 12 h. Haemolymph harvested from silkworms infected with baculovirus was diluted with TC100 medium, and 0.2 ml sample was incubated with BmN cells at 27 °C for 1 h. The supernatant was then removed and cells were covered with 1 % SeaPlaque agarose (Takara) solution in TC100 medium, which was warmed to 40 °C. Cells were cultured further at 27 °C for 5 days. The sample was covered with SeaPlaque solution (2 ml) containing 0.05 mg neutral red $ml^{-1}$, and incubated at 27 °C for 12 h. Plaques were counted under a microscope. To determine inhibitory effects on baculovirus proliferation by antiviral agents, as shown in Fig. 2(e), BmN cells were infected with approximately 100 p.f.u. baculovirus, and antiviral agents were mixed in the agarose solutions. To obtain $IC_{50}$ values of antiviral agents in Table 1, BmN4 cells ($1 \times 10^5$) were infected with $1 \times 10^5$ p.f.u. baculovirus and incubated in TC100 medium containing antiviral agents for 5 days. The p.f.u. level of each culture supernatant was determined by plaque-forming assay, as described above.

**Purification of a compound with antiviral activity from cinnamon bark.** Cinnamon-bark powder (376 g) was extracted sequentially with n-hexane, chloroform, ethylacetate and methanol, and the extracts were evaporated. Extract residues were then dissolved with 0.9 % NaCl containing 5 % DMSO, and the therapeutic effects of the extract were evaluated in silkworms infected by baculovirus. Chloroform fractions (11.8 g) that had a therapeutic effect were fractionated by silica-gel chromatography. Adsorbed compounds bound to the column were eluted sequentially by dichloromethylene, dichloromethylene/methanol (100 : 2) and dichloromethylene/methanol (95 : 5), and the therapeutic effects of each fraction were evaluated. Active fractions (663 mg) were pooled and purified further by Sephadex LH20 (75 g) column chromatography. The column was washed with methanol and 10 ml fractions were collected, followed by evaluation of the therapeutic effect of the fractions. The active fractions were purified further by high-performance liquid chromatography (HPLC; μBondasphere). Materials were eluted with 60 % methanol and then peak fractions, detected with a refractive-index

**Table 1.** $ED_{50}$ and $IC_{50}$ values of antiviral drugs

$ED_{50}$ values were calculated from the results shown in Fig. 1 as the amount of drug required for 50 % survival of silkworms infected with BmNPV. $IC_{50}$ values were determined by inhibition of BmNPV proliferation in BmN4 cells. Mean values from two independent experiments are shown.

| Antiviral drug | $ED_{50}$* [μg (g larva)$^{-1}$] | $IC_{50}$† (μg $ml^{-1}$) | $ED_{50}$ : $IC_{50}$ ratio |
|---|---|---|---|
| Ganciclovir | 31 | 32 | 1.0 |
| Foscarnet | 84 | 105 | 0.8 |
| Vidarabine | 290 | 63 | 4.6 |
| Ribavirin | 10 | 11 | 0.9 |

*Measured in silkworms.
†Measured in BmN4 cultured cells.

detector, were pooled and concentrated, followed by measurement of the therapeutic effects in the silkworm infection model. Active fractions, which were eluted at 15.8 min, were analysed by $^{1}$H nuclear magnetic resonance ($^{1}$H-NMR) and $^{13}$C-NMR at 500 and 125 MHz, respectively.

**Assay for anti-herpes simplex virus type 1 (HSV-1) activity of cinnzeylanine.** Anti-HSV-1 activity was measured by plaque-reduction assay (Tanaka *et al.*, 2004). Vero cells (Tanaka *et al.*, 2003) were grown to the confluent stage in 24-well titre plates, in Dulbecco's modified Eagles medium (Nacalai) supplemented with heat-treated fetal bovine serum (1%). Medium was changed to 0.25 ml 199 medium (Sigma) supplemented with 1% heat-treated fetal bovine serum. HSV-1 F strain (100 p.f.u.) (Ejercito *et al.*, 1968; Kawaguchi *et al.*, 2003) was adsorbed to the cells for 1 h, followed by incubation with 200 µl 199 medium containing 50 mM HEPES/KOH (pH 7.5), test sample and antibody against HSV-1 for 45 h. Cells were fixed with methanol and stained with crystal violet, followed by counting of plaques under a microscope.

**Calculation of $ED_{50}$ and $IC_{50}$ values.** $ED_{50}$ values were calculated by probit analysis. $IC_{50}$ values were determined graphically.

## RESULTS

### Therapeutic effects of antiviral agents against the killing effect of baculovirus in silkworms

Ribavirin, ganciclovir, foscarnet and vidarabine are used clinically to treat virus-infected human patients. These antiviral agents inhibited the proliferation of baculovirus in BmN4 cells, which are derived from silkworms. $IC_{50}$ values were determined as the concentration of these reagents needed to produce 50% inhibition of plaque formation (Table 1). We determined whether these antiviral compounds have therapeutic effects in silkworms infected with baculovirus. When $1.6 \times 10^{4}$ p.f.u. baculovirus was injected into the haemolymph of silkworms, all of the animals died within 5 days (Fig. 1a). Each of the antiviral agents produced a dose-dependent increase in the number of surviving silkworms (Fig. 1b). We calculated the $ED_{50}$ values, i.e. the amount of the agents required to produce a silkworm survival rate of 50% (Table 1). The $ED_{50}$ values obtained were consistent with the amount of the antiviral agents used for clinical administration in humans. Silkworms were still alive after injection of >500 µg of these drugs, indicating that the toxicity of these drugs in silkworms was negligible.

Next, we examined whether these antiviral agents inhibited the proliferation of baculovirus in the body fluid of silkworms. We harvested haemolymph from silkworms and determined the number of viruses by using a plaque-forming assay, and found that the increase in the number of viruses in the haemolymph was inhibited by the antiviral agents (Fig. 1c). These results indicate that the therapeutic effects of these antiviral agents can be explained by the inhibition of viral proliferation in the silkworm body. The results also suggest that silkworms infected with

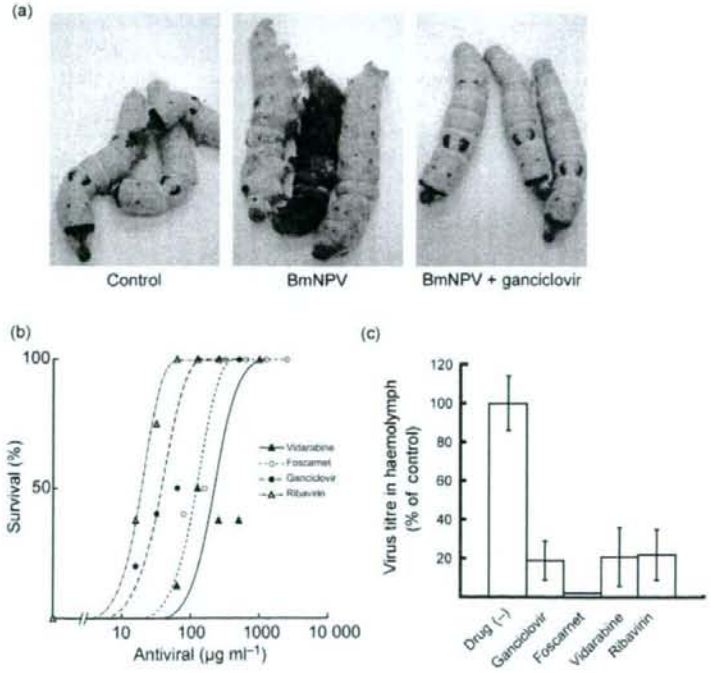


**Fig. 1.** Therapeutic effects of antiviral agents in silkworms infected with baculovirus. (a) Effect of antiviral agents in silkworms infected with baculovirus. Photos show silkworms 120 h after intra-haemolymph administration of saline (left panel), baculovirus (centre panel) or baculovirus+120 µg ganciclovir (right panel). (b) Dose dependence of therapeutic effects of antiviral agents in the silkworm–baculovirus infection model. Ten silkworms were used for each dose of antiviral agents. Consistent results were obtained from three independent experiments. A typical result is shown. (c) Antiviral agent-induced inhibition of baculovirus proliferation in the body fluid of silkworms. Mean values of five to eight infected larvae are shown. Error bars indicate SD.

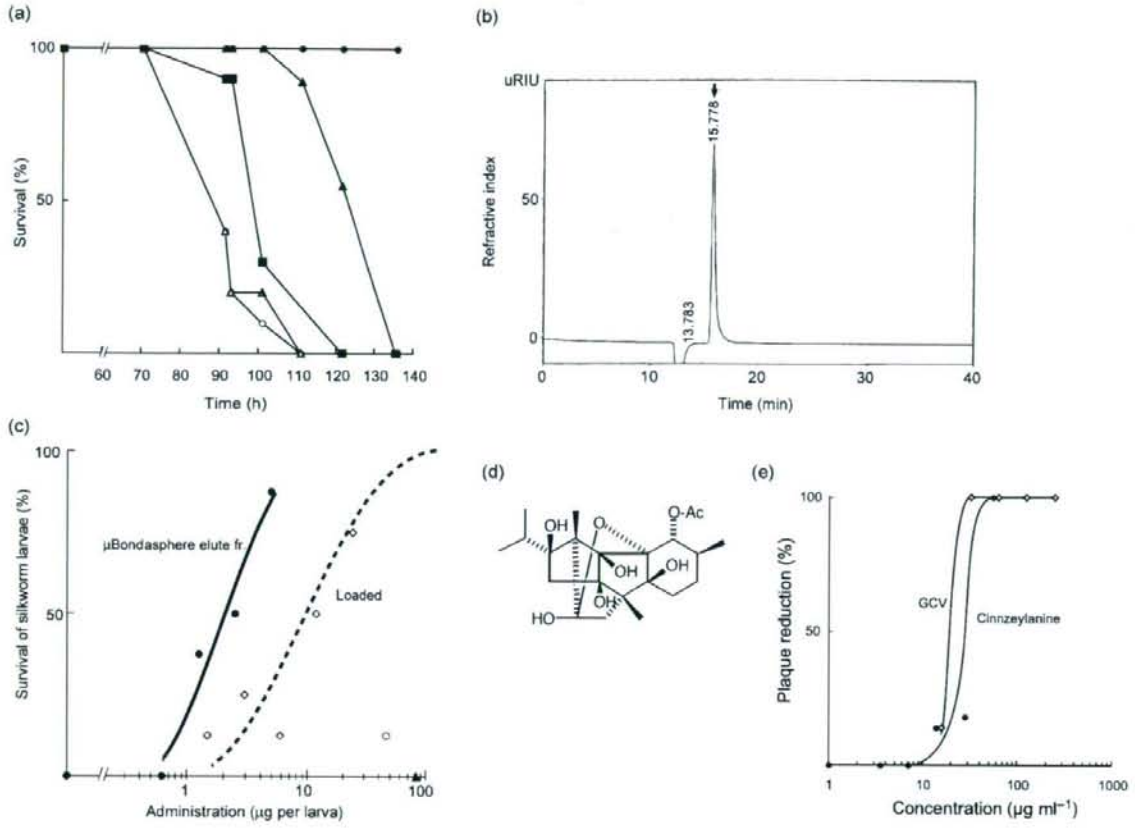


**Fig. 2.** Evaluation of the therapeutic effects of Kampo medicines on baculovirus infection in silkworms, and purification of the antiviral compound from cinnamon bark based on measurement of the therapeutic effect. (a) Therapeutic effect of Kampo medicines in silkworms infected with baculovirus. ●, Control; ○, BmNPV + saline; ▲, BmNPV + Mao-to (100 mg); △, BmNPV + Shosaiko-to (200 mg); ■, BmNPV + Kakkon-to (200 mg). (b) Elution profile of μBondasphere column chromatography, the final step of the purification. (c) Therapeutic effect of the final purified fraction in silkworms infected with baculovirus. (d) Structure of the effective compound, determined by NMR analysis. (e) Ganciclovir (GCV; □)- or cinnzeylanine (●)-induced inhibition of baculovirus proliferation in BmN cells.

baculovirus are a useful model for evaluating the therapeutic effects of antiviral agents.

## Purification of antiviral agent in Kampo medicine based on the therapeutic effects determined by using the silkworm infection model

We speculated that this silkworm–baculovirus infection model would be useful for evaluating new antiviral drugs. Thus, we screened for antiviral agents in natural sources by using this model. We examined the therapeutic effects of Mao-to, Kakkon-to and Shosaiko-to. Mao-to showed positive results (Fig. 2a).

Mao-to is composed of four plant-derived medicines: ephedra herb, apricot kernel, licorice root and cinnamon bark. We examined the therapeutic effects of the hot-water extracts of each crude drug in the silkworm–baculovirus infection model, and found that cinnamon bark had therapeutic activity. We purified the antiviral agent in cinnamon bark further by using the therapeutic assay. The antiviral component was extracted efficiently with chloroform. The chloroform extract was purified further with chromatography using Silicagel C200, Sephadex LH20 and reversed-phase HPLC with μBondasphere (Table 2). The final purification using HPLC with μBondasphere produced a single peak (Fig. 2b), indicating that the fraction was highly homogeneous. The fraction inhibited the proliferation of BmNPV in BmN cultured cells (Fig. 2e). The $ED_{50}$ value of the fraction was 1 μg per larva, which was 190-fold lower than that of the chloroform extract. The $ED_{50}$ value was 3% of that of ganciclovir [31 μg (g

**Table 2.** Summary of the purification of the component of cinnamon bark with antiviral activity

Therapeutic activity was determined by using the silkworm infection model. One unit indicates the amount required for the survival of 50 % of silkworms infected with BmNPV. $ED_{50}$ values were calculated based on the assumption that the mass of the silkworm body was 2 g.

| Fraction | | Activity (units) | Recovery (%) | Weight (mg) | $ED_{50}$ [μg (g larva)$^{-1}$] |
|---|---|---|---|---|---|
| I | $CHCl_3$ extract | 32 000 | 100 | 12 000 | 190 |
| II | C200 column chromatograpy | 11 000 | 35 | 660 | 30 |
| III | LH20 column chromatography | 3 400 | 12 | 34 | 5 |
| IV | μBondasphere column chromatography | 1 000 | 3 | 2 | 1 |

larva)$^{-1}$] in the silkworm–baculovirus infection model (Fig. 2c).

The purified fraction was analysed by $^{1}$H- and $^{13}$C-NMR, and the structure of the compound was determined (Fig. 2d). This compound was identified as cinnzeylanine, which was detected previously in the bark of *Cinnamomum zeylanicum* (Isogai *et al.*, 1977) and *Cinnamomum cassia* (Yagi *et al.*, 1980). The antiviral activity of cinnzeylanine has not been reported previously. Our results are, to our knowledge, the first to demonstrate that cinnzeylanine has a therapeutic effect against baculovirus infection in silkworms.

### Cinnzeylanine inhibition of HSV-1 proliferation in Vero cells

We next examined whether cinnzeylanine inhibited the proliferation of HSV-1, an infectious virus in humans. The effects of various concentrations of cinnzeylanine on the proliferation of HSV-1 in Vero cells, a cell line derived from monkey, were tested by using a plaque-reduction assay (Fig. 3). Cinnzeylanine reduced the number of HSV-1 plaques. The cinnzeylanine concentration that decreased the plaque number by 50 % ($IC_{50}$) was 230 μg ml$^{-1}$. Vero cells remained attached to the culture dish even in the presence of 320 μg cinnzeylanine ml$^{-1}$, which abolished HSV-1-induced plaque formation completely.

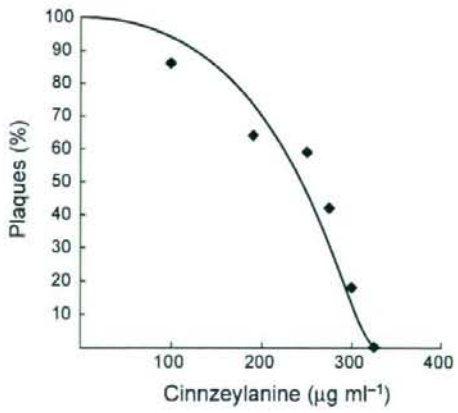


**Fig. 3.** Inhibitory effect of cinnzeylanine on HSV-1 proliferation in Vero cells.

## DISCUSSION

### Evaluation of therapeutic effects of antiviral agents in the silkworm–baculovirus infection model

The present study demonstrated that antiviral agents that are used clinically for treating humans are effective in the silkworm–baculovirus infection model. These antiviral agents, which target DNA polymerase, inhibited the proliferation of baculovirus in cultured cells (Table 1). We consider that the mechanism of action of these antiviral agents is inhibition of the increase in the number of viral particles in infected cells (Fig. 1c). Inhibition of the proliferation of baculovirus by ganciclovir, vidarabine and foscarnet is thought to be due to the inhibition of viral DNA replication. The mechanism of ribavirin for inhibiting baculovirus proliferation is unknown, although ribavirin reportedly acts as a mutagen (Chevaliez *et al.*, 2007; Crotty *et al.*, 2000; Graci *et al.*, 2007) and as an inhibitor of IMP dehydrogenase (Lowe *et al.*, 1977; Parker, 2005). Ribavirin might inhibit the proliferation of baculovirus by these mechanisms.

We suggest that the silkworm–baculovirus infection model is useful for evaluating the therapeutic effects of antiviral agents against DNA viruses. To evaluate the therapeutic effects of compounds against RNA virus infection, including severe acute respiratory syndrome coronavirus and human influenza viruses, further studies of a corresponding RNA virus that infects silkworms are needed. Cytoplasmic polyhedron virus, which is classified as a member of the family *Reoviridae* and contains RNA-dependent RNA polymerase (Hagiwara & Matsumoto, 2000), might be a candidate model virus for reovirus and severe acute respiratory syndrome coronavirus.

Baculovirus does not have a gene encoding a nucleotide kinase that phosphorylates ganciclovir. Therefore, ganciclovir might be phosphorylated by a silkworm cellular kinase, resulting in the inhibition of viral DNA replication, although it is possible that a protein kinase induced by